High-Frequency Volatility Forecasting of US Housing Markets*

Mawuli Segnon†
Department of Economics, Institute for Econometric and Economic Statistics, University of Münster, Germany

Rangan Gupta‡
University of Pretoria, Department of Economics, Pretoria, South Africa

Keagile Lesame§
University of Pretoria, Department of Economics, Pretoria, South Africa

and
Mark E. Wohar¶
Department of Economics, University of NE-Omaha, USA; School of Business and Economics, Loughborough University, UK

Abstract: We propose a logistic smooth transition autoregressive fractionally integrated [STARFI (p,d)] process for modeling and forecasting US housing price volatility. We discuss the statistical properties of the model and investigate its forecasting performance by assuming various specifications for the dynamics underlying the variance process in the model. Using a unique database of daily data on price indices from ten major US cities, and the corresponding daily Composite 10 Housing Price Index, and also a housing futures price index, we find that using the Markov-switching multifractal (MSM) and FIGARCH frameworks for modeling the variance process helps improving the gains in forecast accuracy.

Keywords US housing prices, GARCH processes, MSM processes, Model confidence set

JEL classification C22, C53, C58

*We would like to thank an anonymous referee for many helpful comments. However, any remaining errors are solely ours.

†Mawuli Segnon, Department of Economics, University of Münster, Germany. E-mail: segnon@uni-muenster.de.
‡Rangan Gupta, Department of Economics, University of Pretoria, South Africa. E-mail: gupta.rangan@gmail.com.
§Keagile Lesame, Department of Economics, University of Pretoria, South Africa. E-mail: keagilel@gmail.com.
¶Corresponding author: Mark E. Wohar, Department of Economics, University of NE-Omaha, USA. E-mail: mwohar@unomaha.edu.

1 Introduction

The housing market plays an important role in the economy of the United States (US), since it constitutes a significant share of many households' asset holding and net worth. According to the Financial Accounts data of the US corresponding to the fourth quarter of 2018, residential real estate represents about 83.7% of total household non-financial assets, 28.3% of total household net worth and 24.6% of household total asset.[6] Therefore, as pointed out by Shiller (1998), the risk or volatility of house prices is among the largest personal economic risks faced by the individual. Note that, housing assets differ from financial assets, such as stocks, since they serve the dual role of investment and consumption (Henderson and Ioannides, 1987). Naturally, the effects of housing on savings and portfolio choices are extremely important questions, and hence, understanding the source of the housing market price volatility is important because it has individual portfolio implications, as it affects households' investment decisions regarding tenure choice and housing quantity (Miles, 2008a). Moreover, the housing market affects the economy not only through wealth effects (Case et al., 2013), but also through influences on other markets such as the mortgage market, mortgage insurance and mortgage backed bonds, as well as consumer durables (Miller and Peng, 2006). Finally, knowledge about house price volatility is also an important input into housing policy (Zhou and Haurin, 2010).[7] In light of these points, the variations in the housing market are important to key components of the overall economy and the welfare of the society.

Given this, a growing number of studies have attempted to model and predict volatility (using univariate models and also with econometric frameworks including wide array of factors) at the aggregate and regional (state and metropolitan statistical areas (MSAs)-levels) of the US (see for example, Dolde and Tirtiroglu (2002), Crawford and Fratantoni (2003), Miller and Peng (2006), Miles (2008a), Miles (2008b), Miles (2011), Zhou and Haurin (2010), Elder and Villupuram (2012), Li (2012), Ajmi et al. (2014), Engsted and Pedersen (2014), Barros et al. (2015), Bork and Møller (2015), Fairchild et al. (2015), André et al. (2017), Chen (2017), Nyakabawo et al. (2018)). All these studies find the existence of Autoregressive Conditional Heteroskedasticity (ARCH) and long memory effects in housing price returns volatility, and a relatively good forecasting performance of the Generalized Autoregressive Conditional Heteroskedasticity (GARCH)-type models.

Our objective is to introduce a new class of volatility processes for modeling and forecasting volatility of US housing markets, namely the Markov-switching multifractal (MSM) process, recently introduced by Calvet and Fisher (2004). The multifractal processes originally stem from the statistical physics and have been adapted to finance by Mandelbrot et al. (1997), Calvet and Fisher (2001, 2004) and Lux (2008). The MSM processes successfully find applications in forecasting returns volatility in stock, exchange-rate, and commodity markets and outperform the GARCH-type models at long forecasting horizons. We adopt three different loss functions and the model confidence set (MCS) test to evaluate and compare the MSM forecasting performance with those of GARCH-type models at short and long horizons. The choice of the MSM process is motivated by the previous findings by

[6] See: https://www.federalreserve.gov/releases/z1/20190920/html/b101h.htm.

[7] For example, consider the following case: if low-valued houses' values are relatively volatile, then policies that encourage low-income renter households to become homeowners should be evaluated in light of the house price risk that they would bear.

Crawford and Fratantoni (2003) and Barros et al. (2015) who provide evidence of nonlinearities and long memory properties of house prices. In fact, the unique framework of the MSM model allows for regime switching of heterogenous persistence creating an apparent long memory. These features are relevant for capturing the dynamics underlying the US housing price volatility. In addition, given that the MSM model requires high-frequency data in general, we deviate from the existing studies on volatility of the US housing market, which are based on monthly or quarterly datasets, by using an unique database of house prices available at daily frequency for the 10 major (Boston, Chicago, Denver, Las Vegas, Los Angeles, Miami, New York, San Diego, San Francisco, and Washington D.C.) Metropolitan Statistical Areas (MSAs) of the US, as well as a composite version for proxying the price of house in the country overall. In this regard, a recently developed daily house price futures data is also used for the sake of robustness. Given the importance of housing price volatility, we believe the usage of daily house price data for forecasting US housing market volatility is likely to be more informative to economic agents and policy authorities in making their respective decisions in a timely manner than those derived from low-frequency data. The daily estimates and forecasts of volatility will provide high-frequency leading information to consumers, investors and policymakers, as to where the economy is headed in the future, as researchers could use this information in a nowcasting framework (Banbura et al., 2011) to forecast important decision-making variables that are measured only at lower-frequencies, using mixed data sampling (MIDAS) regressions (see Andreou et al., 2010).

At this stage a caveat is in order.[8] As indicated at the onset, the MSM approach is more suited to high-frequency data, but in general, house price data is not available at a daily frequency when it comes to the coverage of the whole country, i.e., for the various states, MSAs, and also the aggregate US. Moreover, the data that we use is a bit outdated, and even though, we do make use of a more recent data set involving house price futures, the lack of wide-spread coverage of this (Case-Shiller-type) data is a concern, especially when compared to that of the low-frequency data maintained by the Federal Housing Finance Agency (FHFA). This is more so, since the US housing market is known to be heterogenous, and cannot be generalized with a single housing index (Apergis and Payne, 2012; Montañés and Olmos, 2013; Barros et al., 2014; Miles, 2015). Given this, unless new high-frequency house price data becomes available for the states, MSAs, and the overall US, we must be cautious about generalizing our findings. Contingent on the availability of high-frequency house price data, an interesting analysis in the future would be to revisit our results in terms of the superiority of the MSM approach.

The remainder of the paper is organized as follows: Section 2 introduces our data sets. The modeling framework is provided in Section 3. We discuss the statistical properties of our models in Section 4. Forecasting methodologies and empirical results are presented in Section 6, and Section 7 concludes.

[8] We would like to thank an anonymous referee for pointing this out to us.

2 Data analysis

Our data set consists of daily housing price indices for 10 major US MSAs with different start and end dates, namely Boston (5/1/1995 - 11/10/2012), Los Angeles (5/1/1995 - 23/10/2012), Chicago (3/9/1999 - 12/10/2012), Denver (5/5/1999 - 17/10/2012), Miami (3/4/1998 - 15/10/2012), Las Vegas (5/1/1995 - 17/10/2012), San Diego (4/1/1996 - 23/10/2012), San Francisco (5/1/1995 - 18/10/2012), New York (5/1/1995 - 23/10/2012) and Washington D.C. (5/6/2001 - 11/10/2012). This unique data is sourced from Bollerslev et al. (2016), whereby the authors use comprehensive housing transaction data from DataQuick, and then apply the repeat sales method to derive these indices. The data set is downloadable from: http://qed.econ.queensu.ca/jae/datasets/bollerslev001/. Following Wang (2014), we compute the daily Composite 10 Housing Price Index, as a proxy for the aggregate housing price of the US, as a weighted average of the house prices of the 10 MSAs. The specific values of the weights used were Boston (0.212), Chicago (0.074), Denver (0.089), Las Vegas (0.037), Los Angeles (0.050), Miami (0.015), New York (0.055), San Diego (0.118), San Francisco (0.272), and Washington D.C. (0.078), representing the total aggregate value of the housing stock in the 10 MSAs in the year 2000. This aggregate index has the daily sample period of 5/6/2001 - 11/10/2012. Since these indices are a bit outdated, even though they do cover the period of turmoil in the US housing market in the wake of the subprime mortage crisis, we also use the CME-S&P Case-Shiller House Price Index (HPI) Continuous Futures (CS-CME), derived from Datastream as maintained by Thomson Reuters, and covers the period of 2/8/2007 - 29/8/2018. We compute the continuously compounded returns as

$$r_t = \left[\ln(p_t) - \ln(p_{t-1})\right], \tag{1}$$

where p_t denotes the housing price in USD at a time t.

Figs. 1 through 4 depict the time evolution of house price returns for 10 US cities, the aggregate index and their squared returns. The descriptive statistics of our data sets are reported in Table 1. Except for Chicago, Miami and future housing price index, we observe a negative skewness in the data for other major cities. All the data sets are characterized by excess kurtosis suggesting a deviation from the normality. This observation can be confirmed by the Jarque-Bera test, which rejects the null hypothesis of the normality at all significant levels. The ARCH test for heteroscedasticity at lag 1 rejects the null of no conditional heteroscedasticity in the data. The results of the augmented Dickey-Fuller (ADF) unit-root test of Dickey and Fuller (1979) and its modified version to account for serial correlations (Phillips-Perron test) in Phillips and Perron (1988) reject the null hypothesis of unit-root. We also apply the KPSS test for stationarity to confirm the verdict of the unit root tests.

We investigate the long memory effects in the US housing price changes by adopting the Detrended Fluctuation Analysis (DFA) (see Weron, 2002) to compute the Hurst exponent indices (see, Table 1). The Hurst indices help to quantify the degree of persistence in data and serve as standard measures of long-term dependence. Except for Las Vegas, San Francisco, U.S. Aggregate and future housing price changes the values for log-price changes are close to 0.5, implying absence of long memory features in housing price returns. For absolute and squared returns the Hurst index values are significantly above 0.5, indicating the presence of long memory in housing price volatility.

We also compute the so-called Hill estimator for the tail index (cf. Hill, 1975) in order to quantify the decay of the unconditional distribution of housing price returns in its extremal region. The estimate for the tail index (see Table 1) is in the vicinity of 3 or above and this result is in harmony with typical findings for financial assets, (see Lux and Ausloos, 2002). Again, this is a clear indication of non-Normality as the slow decay of the distribution of returns implies that large price changes occur with much higher probability than under a Gaussian shape.

We also investigate the nonlinearity in the mean process using the White (see Lee et al., 1993) and Teraesvirta neural network tests (see, Table 1). Based on the results of Teraesvirta neural network test (see Teraesvirta et al., 1993) only Las Vegas, San Diego and San Francisco exhibit linearity in "mean". These results confirm that U.S. housing price indices are characterized by nonlinearities.

Figs. 5 through 8 show the autocorrelation functions for log-returns and squared log-returns. We observe that the squared log-returns are highly correlated. However, the Ljung-Box tests also reject the null hypothesis of no serial correlation for log-returns at the 5% significance level for Denver and San Diego. This indicates the presence of some serial dependence and predictability in the returns of housing prices for those cities. Overall, the U.S. housing price indices, therefore, share the typical salient features of financial assets that are captured by the catchwords "fat tails" and "clustered volatility", but some of them show some deviation from the "efficiency" of stock or foreign exchange markets (their complete lack of predictability). These findings have motivated the choice of our proposed processes.[9]

3 Modeling framework

We assume that returns $\{r_t\}$ in US housing markets follow a smooth transition autoregressive fractionally integrated process [STARFI(p, d)] that satisfies the following equation:

$$\Phi_{s_t;\eta}(L)(1-L)^d r_t = \epsilon_t, \tag{2}$$

where $\epsilon_t|\Omega_{t-1} \sim N(0, \sigma_t^2)$.

Ω_{t-1} is the $\sigma-$field generated by the past information $\{\epsilon_{t-1}, \epsilon_{t-2}, \dots\}$. The lag polynomials in *Eq.* 2 are defined as: $\Phi_{s_t;\eta}(L) = 1 - \phi_1(s_t;\eta_1)L - \cdots - \phi_p(s_t;\eta_p)L^p$ where the autoregressive coefficients $\phi_i(s_t, \eta_i) = \phi_{i0} + \phi_{i1}G(s_t, \tau, c))$, for $i = 1, \dots, p$, are nonlinear functions that have to be defined, s_t denotes the state variable and $\eta_i = (\phi_{i0}, \phi_{i1}, \tau, c)'$ a vector of parameters, and d is a real number. L is the lag operator and $(1-L)^d$ is the fractional differencing operator that is given by

$$(1-L)^d = \sum_{k=0}^{\infty} \frac{\Gamma(k-d)L^k}{\Gamma(-d)\Gamma(k+1)}, \tag{3}$$

with $\Gamma(\cdot)$ being the gamma function.

The transition function $G(s_t, \tau, c)$ follows the first-order Logistic function that is given:

[9] It must be realized that, the features of efficiency, long-memory, nonlinearity, and non-normality, as observed traditionally for other asset markets, are however not likely due to the usage of high-frequency data of the housing market. In fact, these features have also been reported for low- frequency (monthly, quarterly, and annual) data for the US by studies such as Canarella et al. (2012) Barros et al. (2015), Balcilar et al. (2015), Gupta and Majumdar (2015), Canarella et al. (2019).

$$G(s_t, \tau, c) = \frac{1}{1 - \exp(-\tau(s_t - c))}, \qquad \tau > 0. \tag{4}$$

Remark. *The STARFI(p,d) reduces to the STAR(p) when* $d = 0$. *The logistic function exhibits the following properties:* $\lim_{s_t \to -\infty} G(s_t, \tau, c) = 0$, $\lim_{s_t \to \infty} G(s_t, \tau, c) = 1$, $G(s_t, 0, c) = 1/2$, $\lim_{\tau \to -\infty} G(s_t, \tau, c) = 0$ *and* $\lim_{\tau \to \infty} G(s_t, \tau, c) = 1$.

In general, the innovation process, ϵ_t, in *Eq.* (2) can be modeled as follows:

$$\epsilon_t = u_t \sigma_t, \tag{5}$$

where u_t is a sequence of independent identically distributed normal random variables with zero mean and unit variance.

Our findings in Section 2 show that US housing markets share the same salient features of financial assets. In addition, the recent research findings in modeling and forecasting financial market volatility that the Markov-switching multifractal (MSM) model can better reproduce the stylized facts of financial markets and provides more accurate forecast than the GARCH-type models. Motivated by all these facts, we choose the MSM and GARCH-type processes for capturing the time-varying dynamics of σ_t:

1. *Markov-switching multifractal (MSM) model*:
   In this framework we assume that the dynamics underlying the housing markets volatility are driven by a hidden Markov chain vector, M_t, that consists of k independent random volatility components, $M_t^{(1)}, M_t^{(2)}, \ldots, M_t^{(k)}$, and the volatility is formalized as:

$$\sigma_t = \bar{\sigma} \sqrt{\prod_{j=1}^{k} M_t^{(j)}}, \tag{6}$$

   where $\bar{\sigma}$ is a scaling factor and k the number of volatility components.

   The dynamics governing the random volatility components (also called multipliers) determines the unique framework that characterizes the multifractal models. At date t, each multiplier $M_t^{(j)}$ is drawn from the base distribution F_M (to be specified) with positive support and unit expectation. Depending on its rank within the hierarchy of multipliers, $M_t^{(j)}$ changes from one period to the next, with probability γ_j, and remains unchanged with probability $1-\gamma_j$, providing a spectrum of low and high frequencies of multiplier renewal.

   The k transition probabilities are are specified as

$$\gamma_j = 2^{j-k}, \qquad j = 1, \ldots, k. \tag{7}$$

   The transition matrix related to the jth multiplier is given by

$$P_j = \begin{pmatrix} 1 - 0.5\gamma_j & 0.5\gamma_j \\ 0.5\gamma_j & 1 - 0.5\gamma_j \end{pmatrix}.$$

To finalize the specification of the MSM model we draw each multiplier, $M_t^{(j)}$ (in the event of a change) from a two-point distribution with support $\{m_0, 2 - m_0\}$, $1 < m_0 < 2$, and probability 0.5, implying the unconditional expectation $\mathbb{E}(M_t^j) = 1$. The transition matrix of the vector $M_t \equiv (M_t^{(1)}, \ldots, M_t^{(k)})'$ becomes the $2^k \times 2^k$ matrix $P = P_1 \otimes P_2 \otimes \cdots \otimes P_k$, where $\otimes$ denotes the Kronecker product. Using the binomial base distribution[10] for the single multipliers implies the finite support $\Gamma \equiv \{m_0, 2 - m_0\}^k$ for M_t and allows implementing of the maximum likelihood approach.

Remark. *A higher k increases the number of regimes (which is 2^k), and generates proximity to long memory over a longer number of lags, but comes at an additional computational cost in our maximum likelihood approach. In contrast to the traditional Markov switching models, in which the number of parameters to be estimated doubles with an additional regime, the number of parameters in MSM model remains constant with an increasing number of regimes. We note that the non-parametric specification of the transition probability does not guarantees the convergence of the process in continuous time limit. Furthermore, we point out that the MSM processes exhibit only* apparent *long memory with an asymptotic hyperbolic decay of the autocorrelation of absolute powers over a finite horizon and does not obey the traditional definition of long memory (see Beran, 1994).*

2. *GARCH-type models*:

   - A more general class of short-memory GARCH(1, 1) models proposed by He and Terasvirta (1999) can be formalized as

$$\sigma_t^\kappa = g(\epsilon_{t-1}) + c(\epsilon_{t-1})\sigma_{t-1}^\kappa, \tag{8}$$

     with $Pr(\sigma_t^\kappa > 0) = 1$, $\kappa > 0$, and where $\{\epsilon_t\}$ is a sequence of i.i.d. standard normal random variables, and $g(x), c(x)$ are nonnegative functions. This class of GARCH-type models includes, among others, the specifications of Bollerslev (1986) (standard GARCH), Glosten et al. (1993) (GJR-GARCH), Nelson (1991) (EGARCH), and Ding et al. (1993) (APARCH). These models are robust and able to capture the most stylized facts of US housing markets.

   - Motivated by the properties observed in log changes of US housing prices and the findings in Barros et al. (2015) we also adopt the FIGARCH model developed by Baillie et al. (1996) that generalizes the standard GARCH framework by introducing fractional differences in the GARCH process and thereby enables the model to reproduce the long-term dependence of US housing price volatility as documented in the high Hurst coefficients of absolute and squared returns. The conditional variance in the FIGARCH(1,d,1) model can be formalized as

$$\sigma_t^2 = \omega + \left[1 - \beta(L) - \phi(L)(1 - L)^d\right]\epsilon_t^2 + \beta\sigma_{t-1}^2, \tag{9}$$

[10] Liu et al. (2007) find that assuming other base distributions, such as lognormal and gamma, makes little difference in empirical applications

where $\omega > 0$, $\phi < 1, \beta < 1, 0 \leq d \leq 1$. L denotes the lag operator and d is the parameter of fractional differentiation. The parameters have to fulfill the following conditions:

$$\beta - d \leq \phi \leq \frac{(2-d)}{3} \tag{10}$$

and

$$d\left[\phi - \frac{(1-d)}{2}\right] \leq \beta(d - \beta + \phi). \tag{11}$$

Remark. *We refer the readers to Conrad and Haag (2006) for generalized restrictions on the parameters in the FIGARCH model. Long-term dependence shows up in the fact, that, in principle, all available past data should be used in the construction of forecasts of future volatility (while in GARCH, its short-term dependence makes it sufficient to use the filtered realization of the conditional variance, σ_t, at the forecast origin, time t).*

4 Statistical properties

In this section we show that our proposed models for modeling and forecasting US housing market volatility are stationary, ergodic and exhibit high-order moments.

Assumption 1. *The roots of the characteristic polynomials $\Phi_{s_t;\eta}(L)$ lie outside the unit circle, the parameter $d \in (-0.5, 0.5)$ and the logistic transition function is well defined.*

Assumption 2. *The random volatility components $M_t^1, M_t^2, \ldots, M_t^k$ with $E(M_t^j) = 1$, $j = 1, \ldots, k$, are nonnegative and independent of each other at any time and $\gamma_j \in (0, 1)$.*

Proposition 1. *Under Assumption 1 and 2, the STARFI(p, d)-MSM(k) model given by 2, 6 and 7 has a unique, second-order stationary solution. It follows that $\{r_t, \epsilon_t, \sigma_t\}$ are strictly stationary, ergodic and invertible.*

Proof. Under Assumption 2, the conditions of *Theorem* 1 in (Chapter 1, section 12 Shiryaev, 1995) are satisfied. It follows that the chain underlying the dynamics of multipliers M_t^j is geometrically ergodic. The ergodic distribution is given by $\pi_l = 1/2^k$, $l = 1, \ldots, 2^k$. Under Assumptions 1 and 2, $\{r_t, \epsilon_t, \sigma_t\}$ are strictly stationary, ergodic and invertible. ■

Proposition 2. *Under Assumption 1, the STARFI(p,d)-GARCH-class model given by 2, 5 and 8 has a unique, $\alpha\delta-$order stationary solution. It follows that $\{r_t, \epsilon_t, \sigma_t\}$ are strictly stationary, ergodic and invertible.*

Proof. Under Assumption 1 and the conditions of *Theorem* 2.1 in Ling and McAleer (2002) with a constant mean process replaced by a stationary univariate STARFI(p,d) process, $\{r_t, \epsilon_t, \sigma_t\}$ are strictly stationary, ergodic and invertible. ■

Proposition 3. *Under Proposition 2, it follows that the $2mth$ moments of $\{r_t, \epsilon_t\}$ are finite, where m is a strictly integer.*

Proof. Under Proposition 1 and the conditions of Theorem 1 in (Chapter 1, section 12 Shiryaev, 1995), the $2mth$ moments of $\{r_t, \epsilon_t\}$ are finite. $b > 1$, it is obvious that all the elements of the transition matrix of the chain underlying the multipliers are strictly positive, $\gamma_j \in (0, 1)$ ■

Proposition 4. *Under Proposition 2, it follows that the mδth moments of the* $\{r_t, \epsilon_t\}$ *exist.*

Proof. Under Proposition 2 and the conditions of Theorem 2.2 in Ling and McAleer (2002), the $m\delta th$ moments of the $\{r_t, \epsilon_t\}$ exist. ■

Denoting $\rho(n) = cov(r_t, r_{t-n})/var(r_t)$ the autocorrelation function of the process defined by *Eq.* 2. $\rho_q(n) = cov(|\epsilon_t|^q, |\epsilon_{t-n}|^q)/var(|\epsilon_t|^q)$ the autocorrelation of ϵ_t for every moment q and every integer n. Consider two arbitrary numbers κ_1 and κ_2 in the open interval $(0, 1)$. The following set of integers $S_k = \{n : \kappa_1 k \leq \log 2(n) \leq \kappa_2 k\}$ contains a large range of intermediate lags.

Proposition 5. *Under Assumption 1, it follows that* $\rho(n) \sim c|n|^{2d-1}$ *as* $n \to \infty$*, where c is a constant.*

Proof. Under Proposition 2 and Theorem 2.4 in Hosking (1981), $\rho(n)$ is proportional to $|n|^{2d-1}$. ■

Proposition 6. *Under Assumption 2, it follows that* $\ln \rho_q(n) \sim -\psi(q) \ln n$ *as* $k \to \infty$*, where* $\psi(q) = \log_2 \left(\frac{E(M^q)}{[E(M^{q/2})]^2} \right)$.

Proof. Under Proposition 2 and the proof of the Proposition 1 in Calvet and Fisher (2004), $\rho(n)$ is proportional to $\psi(q) \ln n$. ■

Remark. *The MSM processes exhibit only* apparent *long memory with an asymptotic hyperbolic decay of the autocorrelation of absolute powers over a finite horizon and does not obey the traditional definition of long memory, that means, asymptotic power-law behavior of autocorrelation functions in the limit or divergence of the spectral density (Beran, 1994).*

Remark. *We note that the FIGARCH process is not covariance stationary. However, there exist many attempts to demonstrate the strict stationarity of the FIGARCH process with infinity variance. We refer the reader to Bougerol and Picard (1992), Giraitis et al. (2000), Kazakevicius and Leipus (2002) and Douc et al. (2008) for more details.*

5 Estimation

We estimate all the models using the maximum likelihood approach. Given the fact that u_t in *Eq.* 5 is assumed to follow a standard normal distribution, the information matrix of the STARFI-GARCH-type models and STARFI-MSM model are bock-diagonal and allow to estimate the models using a two-stage procedure without loss of efficiency (see Lundbergh and Terasvirta, 1999). In the first stage we adopt the Non-linear Squares (NLS) to estimate the parameters of the conditional mean process. The optimal lag p in STARFI model is determined based on the Akaike information criterion. We note that here that under normality assumption the NLS is equivalent to MLE (Wooldridge, 1994).

Remark. *Based on the fact that under assumption 1, the STARFI process defined in* Eq. 2 *is strictly stationary and ergodic and the necessary and sufficient conditions for the existence of moments are satisfied, the* $\hat{\epsilon}_t$ *are the consistent estimates of the* ϵ_t *(see Chan and McAleer, 2002).*

In the second stage we use the computed residuals to estimate the parameters of the conditional variance via the maximum likelihood method. In the GARCH-type models we fix the optimal lag $p = q = 1$. It well documented that using $p = q = 1$ is enough to effectively capture the dynamics underlying the variance process (see Bollerslev et al., 1994). The parameters are well-estimated and asymptotically efficient. To save place we do not report them, but can be submitted under request.

6 Empirical study

We investigate the forecasting performance of our models using three loss functions, namely the root mean squared error, mean absolute error and the value-at-risk (VaR) based loss function. In addition, we apply the model confidence set (MCS) test of Hansen et al. (2011) to identify models that perform well in our portfolio of models. We adopt a rolling forecasting scheme that consists of removing one earlier observation and adding a new one day by day, so that the estimation sample size remains constant over the out-of-sample. For all 10 US cities and their composite index we use observations until 31/12/2007 as in-sample and those from 01/01/2008 to the end of each data set as out-sample. For each run, we produce forecasts up to 20 days ahead. For house price futures data set we take the first half of the observations as in-sample and the remaining as out-of-sample.

6.1 Forecasting evaluation criteria

The root mean square error, the mean absolute deviation and the mean of the VaR-based loss function that are given by

$$\mathrm{RMSE}_h^{j,k} = \left(\frac{1}{n} \sum_{i=1}^{n} \left(\sigma^2_{T+i,h,k} - \hat{\sigma}^2_{T+i,h,j,k} \right)^2 \right)^{1/2}, \tag{12}$$

$$\mathrm{MAE}_h^{j,k} = \frac{1}{n} \sum_{i=1}^{n} |\sigma^2_{T+i,h,k} - \hat{\sigma}^2_{T+i,h,j,k}|, \tag{13}$$

and

$$\mathrm{MVaR}_h^{j,k}(\alpha) = n^{-1} \sum_{i=1}^{n} \left(\alpha - I^{\alpha}_{T+h,j,k} \right) \left(\epsilon_{T+h,j,k} - VaR^{\alpha}_{T+h,j,k} \right), \tag{14}$$

respectively. j denotes a particular model in our portfolio and k represents a particular U.S. city or index, n is the number of out-sample forecast observations, T the forecast origin and h the forecasting horizon. $\hat{\sigma}^2_{T+i,h,j,k}$ denotes the volatility forecast obtained using a GARCH-type model or MSM model, $\sigma^2_{T+i,h,k}$ is the daily actual volatility that is approximated by the daily squared returns, $I^{\alpha}_{T+h,j,k} = \mathbf{1}(\epsilon_{T+h,j,k} < VaR^{\alpha}_{T+h,j,k})$, $VaR^{\alpha}_{T+h,j,k} = F^{-1}_{T+h}(\alpha)\hat{\sigma}_{T+h,j,k}$ is the conditional value-at-risk, and $F_{T+h}(.)$ is the forecast cumulative distribution of the standardized returns. As with RMSE and MAE, a smaller value for the MVaR(α) points to a good predictive performance. VaR forecasts provide an assessment of the loss that occurs in the α percent worst cases, and are used to determine the necessary level of underlying equity for risky assets to cover the risk of extreme market movement. The asymmetry of (14) helps to avoid making type I-errors (failing to forecast a large negative change) to be more important than issuing an erroneous warning signal.

We note that the VaR-based loss function defined in *Eq.* (14) is not differentiable due to the presence of the indicator function. The non-differentiability of MVaR(α) may cause a problem in the implementation of the MCS test of Hansen et al. (2011) that is based on the framework of White (2000). To obtain consistent results we also use a smooth approximation[11] to MVaR(α), denoted as MSVaR(α), that is differentiable and given by

$$\text{MSVaR}_h^{j,k}(\alpha) = n^{-1} \sum_{i=1}^{n} \left[\alpha - g_\nu\left(\epsilon_{T+h,j,k}, VaR^{\alpha}_{T+h,j,k}\right)\right]\left(\epsilon_{T+h,j,k} - VaR^{\alpha}_{T+h,j,k}\right), \tag{15}$$

$g_\nu(y,z) = [1 + \exp(\nu(y-z))]^{-1}$. The parameter, $\nu > 0$, governs the smoothness and for a higher value of ν MSVaR(α) gets closer to MVaR(α).

To draw meaningful inferences about the relative forecasting performance of our proposed models for forecasting housing market volatility, we apply the model confidence set (MCS) test that was recently developed by Hansen et al. (2011). The basic idea of the MCS approach is to derive from an initial set of competing models, $\mathcal{M}_0$ without a predefined benchmark model, a set of superior models, $\mathcal{M}^*$ at forecasting horizon h, with a given confidence level. Formally, we have

$$\mathcal{M}^* = \{i \in \mathcal{M}_0 | \, \mathbb{E}\left(d^h_{i,j}\right) \leq 0 \; \forall j \in \mathcal{M}_0\},$$

where $d^h_{i,j} = L_{i,h} - L_{j,h}$ is the loss differential between models i and j. $L_{i,h}$ denotes a specific loss function of a particular model i. Based on the expected loss functions, competing models are ranked and the worst performing model at each step is eliminated. This sequential elimination continues until the null hypothesis of equal loss differentials for all models cannot be rejected:

$$H_0 : \mathbb{E}\left(d^h_{i,j}\right) \leq 0 \; \forall i, j \in \mathcal{M}.$$

The test statistic used under the null is either the range statistic, T_r, or the semi-quadratic statistic, T_{sq}, that are given by

$$T_r = \max_{i,j \in \mathcal{M}} \frac{|\bar{d}_{i,j}|}{\sqrt{v\hat{a}r(\bar{d}_{i,j})}}, \quad T_{sq} = \sum_{i \neq j} \frac{(\bar{d}_{i,j})^2}{\sqrt{v\hat{a}r(\bar{d}_{i,j})}}.$$

The p-values can easily be obtained via a stationary bootstrap procedures that are developed based on the framework in White (2000). We refer the reader to Hansen et al. (2011) for details on the framework of the MCS approach concerning the impact of the (i) forecasting schemes used, (ii) the relationships between models under comparison and (iii) the differentiation of the loss functions used.

6.2 Forecasting results

Tables 2 through 4 report MSE, MAE, MVaR(1%) and MSVaR(1%) of housing price volatility forecasts for our six volatility models used in this analysis and across US cities or indices. For the MCS test we have used both the differentiable and non-differentiable VaR-based loss function. We only

[11] As mentioned by Granger (1999) the issue associated with the non-differentiability may be just a technicality due to the fact that it should always be possible to find a smooth function which is arbitrarily close to the non-smooth one.

report the MCS test results for $\nu \geq 6950$. The p-values of the MCS test and the rank of the models are reported in Table 5 through 10.

Based on the RMSE criterion, all the models perform well at different forecasting horizons and across all indices. However, based on the MCS test results we observe that in most cases the MSM model clearly outperforms other competitive models at the 1-day forecasting horizon. At the 10-days forecasting horizon and beyond the MCS test results indicate that for Denver, Las Vegas all the volatility models are in the optimal set at the 95% confidence level suggesting that for these US cities all models perform equally well.

According to the MAE criterion and the MCS test results, FIGARCH seems to be the best model followed by the MSM model across indices and performs better than short-memory GARCH-type models at the different horizons. Based on the MVaR(1%) criterion and the MCS test results the MSM model outperforms its competitors at the 10-days ahead and beyond across all indices. The second best model seems to be the EGARCH model. Note that the differences in forecasting performance between the MSM and GARCH-type models across US cities or indices appear so pronounced under the MVaR criterion. The MSM model provides better average MVaR results and as for the smooth MSVaR criterion, practically no differences are detected compared to the non-differentiable MVaR as the smoothness parameter ν increases.

7 Conclusion

In this paper we have shown that the US housing markets share the typical salient features of financial assets. However, we note that the persistence in US housing markets is more pronounced and that the tails have more probability mass than observed in the stock, foreign exchange and commodity markets. We have proposed various approaches for modeling and forecasting US housing market volatility and discussed the statistical properties of the models used. We have evaluated and compared the out-of-sample forecasting ability of the models via three loss functions and the model confidence set (MCS) test. We found that based on the RMSE criterion all models in most cases perform well. Using the asymmetric loss functions such as the MAE and MVAR, the MSM followed by the FIGARCH outperform the short-memory GARCH-type models.

References

Ajmi, A. H., V. Babalos, F. Economou, and R. Gupta (2014). Real estate market and uncertainty shocks: A novel variance causality approach. *Frontiers in Finance and Economics 2*, 56–85.

André, C., L. Bonga-Bonga, R. Gupta, and J. W. M. Mwamba (2017). Economic policy uncertainty, us real housing returns and their volatility: A nonparametric approach. *Journal of Real Estate Research 39*, 493–513.

Andreou, E., E. Ghysels, and A. Kourtellos (2010). Regression models with mixed sampling frequencies. *Journal of Econometrics 158*, 246–261.

Apergis, N. and J. E. Payne (2012). Convergence in U.S. housing prices by state: Evidence from the club convergence and clustering procedure. *Letters in Spatial and Resource Sciences 5*, 103–111.

Baillie, R. T., T. Bollerslev, and H. O. Mikkelsen (1996). Fractionally integrated generalized autoregressive conditional heteroskedasticity. *Journal of Econometrics 74*, 3–30.

Balcilar, M., R. Gupta, and S. M. Miller (2015). The out-of-sample forecasting performance of nonlinear models of regional housing prices in the US. *Applied Economics 47*, 2259–2277.

Banbura, M., D. Giannone, and L. Reichlin (2011). *Oxford Handbook on Economic Forecasting*, Chapter Nowcasting, pp. 63–90. Oxford University Press.

Barros, C. P., L. A. Gil-Alana, and J. E. Payne (2014). Tests of convergence and long memory behavior in u.s. housing prices by state. *Journal of Housing Research 23*, 73–88.

Barros, C. P., L. A. GilAlana, and J. E. Payne (2015). Modeling the long memory behavior in U.S. housing price volatility. *Journal of Housing Research 24*, 87–106.

Barros, P. C., L. A. Gil-Alana, and J. E. Payne (2015). Modeling the long memory behavior in U.S. housing price volatility. *Journal of Housing Research 24*, 87–106.

Beran, J. (1994). *Statistics for Long-memory Processes*. New York: Chapman and Hall.

Bollerslev, T. (1986). Generalized autoregressive conditional heteroskedasticity. *Journal of Econometrics 31*, 307–327.

Bollerslev, T., R. F. Engle, and D. Nelson (1994). *Handbook of Econometrics*, Volume 4, Chapter ARCH models, pp. 2961–3038. Elsevier Science BV, Amsterdam.

Bollerslev, T., A. Patton, and W. Wang (2016). Daily house price index: Construction modelling and longer-run predictions. *Journal of Applied Econometrics 31*, 1005–1025.

Bork, L. and S. V. Møller (2015). Forecasting house prices in the 50 states using dynamic model averaging and dynamic model selection. *International Journal of Forecasting 31*, 63–78.

Bougerol, P. and N. Picard (1992). Stationarity of GARCH processes and of some nonnegative time series. *Journal of Econometrics 52*, 115–127.

Calvet, L. and A. Fisher (2001). Forecasting multifractal volatility. *Journal of Econometrics 105*, 27–58.

Calvet, L. and A. Fisher (2004). Regime-switching and the estimation of multifractal processes. *Journal of Financial Econometrics 2*, 44–83.

Canarella, G., L. A. Gil-Alana, R. Payne, and S. M. Miller (2019). Persistence and cyclical dynamics of US and UK house prices: Evidence from over 150 years of data. *Urban Studies*. DOI: https://doi.org/10.1177/0042098019872691.

Canarella, G., S. M. Miller, and S. K. Pollard (2012). Unit roots and structural change: An application to US house-price indices. *Urban Studies 49*, 757–776.

Case, K. E., J. M. Quigley, and R. J. Shiller (2013). Wealth effects revisited 1975-2012. *Critical Finance Review 2*, 101–128.

Chan, F. and M. McAleer (2002). Maximum likelihood estimation of STAR and STAR-GARCH models: Theory and monthe carlo evidence. *Journal of Applied Econometrics 17*, 509–534.

Chen, H. (2017). Real estate transfer taxes and housing price volatility in the United States. *International real Estate Review 20*, 207–219.

Conrad, C. and B. R. Haag (2006). Inequality constraints in the fractionally integrated GARCH model. *Journal of Financial Econometrics 4*, 413–449.

Crawford, F. W. and M. C. Fratantoni (2003). Assessing the forecasting performance of regime switching ARIMA and GARCH models of home prices. *Real Estate Economics 31*, 223–243.

Dickey, D. A. and W. A. Fuller (1979). Distribution of the estimators for autoregressive time series with a unit root. *Journal of the American Statistical Association 74*, 427–431.

Ding, Z., C. Granger, and R. Engle (1993). A long memory property of stock market returns and a new model. *Journal of Empirical Finance 1*, 83–106.

Dolde, W. and D. Tirtiroglu (2002). House price volatility changes and their effects. *Real Estate Economics 30*, 41–66.

Douc, R., F. Roueff, and P. Soulier (2008). On the existence of some ARCH(∞) processes. *Stochastic Processes and Applications 118*, 755–761.

Elder, J. and S. Villupuram (2012). Persistence in the return and volatility of home price indices. *Applied Financial Economics 22*, 1855–1868.

Engsted, T. and T. Q. Pedersen (2014). Housing market volatility in the OECD area: Evidence from VAR based return decompositions. *Journal of Macroeconomics 42*, 91–103.

Fairchild, J., J. Ma, and S. Wu (2015). Understanding housing market volatility. *Journal of Money Credit and Banking 47*, 1309–1337.

Giraitis, L., P. Kokoszka, and R. Leipus (2000). Stationarity ARCH models: Dependence structure and central limit theorem. *Econometric Theory 16*, 3–22.

Glosten, L., R. Jagannathan, and D. E. Runkle (1993). On the relation between the expected value and volatility of the nominal excess return on stocks. *Journal of Finance 46*, 1779–1801.

Granger, C. W. (1999). Outline of forecast theory using generalized cost functions. *Spanish Economic Review 1*, 161–173.

Gupta, R. and A. Majumdar (2015). Forecasting US real house price returns over 1831-2013: evidence from copula models. *Applied Economics 47*, 5204–5213.

Hansen, P. R., A. Lunde, and J. M. Nason (2011). The model confidence set. *Econometrica 79*, 453–497.

He, C. and T. Terasvirta (1999). Properties of moments of a family of GARCH processes. *Journal of Econometrics 92*, 173–192.

Henderson, J. V. and Y. Ioannides (1987). Owner occupancy: Consumption vs. investment demand. *Journal of Urban Economics 21*, 228–241.

Hill, B. M. (1975). A simple general approach to inference the tail of a distribution. *Annals of Statistics 3*, 1163–1174.

Hosking, J. R. (1981). Fractional differencing. *Biometrika 68*, 165–176.

Kazakevicius, V. and R. Leipus (2002). On stationarity in the ARCH(∞) model. *Econometric Theory 18*, 1–16.

Lee, T. H., H. White, and C. W. J. Granger (1993). Testing for neglected nonlinearity in time series models. *Journal of Econometrics 56*, 269–290.

Li, K.-W. (2012). A study on the volatility forecast of the US housing market in the 2008 crisis. *Applied Financial Economics 22*, 1869–1880.

Ling, S. and M. McAleer (2002). Necessary and sufficient moment conditions for the GARCH(r,s) and asymmetric power GARCH(r,s) models. *Econometric Theory 18*, 722–729.

Liu, R., T. di Matteo, and T. Lux (2007). True and apparent scaling: The proximity of the Markov-switching multifractal model to long-range dependence. *Physica A 383*, 35–42.

Lundbergh, S. and T. Terasvirta (1999). Modelling economic high frequency time series with STAR-STGARCH models. SSE/EFI Working Paper Series in Economics and Finance, No. 291.

Lux, T. (2008). The Markov-switching multifractal model of asset returns: GMM estimation and linear forecasting of volatility. *Journal of Business and Economic Statistics 26*, 194–210.

Lux, T. and M. Ausloos (2002). Market fluctuations I: Scaling, multi-scaling and their possible origins. In A. Bunde, J. Kropp, and H.-J. Schellnhuber (Eds.), *Science of Disasters: Climate Disruptions, Heart Attacks and Market Crashes*, pp. 372–409. Springer, Berlin.

Mandelbrot, B. B., A. Fisher, and L. Calvet (1997). A multifractal model of asset returns. Cowles Foundation Discussion Papers 1164, Cowles Foundation for Research in Economics, Yale University.

Miles, W. (2008a). Boom-bust cycles and the forecasting performance of linear and non-linear models of house prices. *Journal of Real Estate Finance and Economics 36*, 249–264.

Miles, W. (2008b). Volatility clustering in U.S. home prices. *Journal of Real Estate Research 30*, 73–90.

Miles, W. (2011). Long range dependence in U.S. house prices volatility. *Journal of Real Estate Finance and Economics 42*, 214–240.

Miles, W. (2015). Regional house price segmentation and convergence in the US: A new approach. *Journal of Real Estate Finance and Economics 50*, 113–128.

Miller, N. G. and L. Peng (2006). Exploring metropolitan price volatility. *Journal of Real Estate Finance and Economics 33*, 5–18.

Montañés, A. and L. Olmos (2013). Convergence in US house prices. *Economics Letters 121*, 152–155.

Nelson, D. B. (1991). Conditional heteroskedasticity in asset returns: A new approach. *Econometrica 59*, 347–370.

Nyakabawo, W., R. Gupta, and H. A. Marfatia (2018). High frequency impact of monetary policy and macroeconomic surprises on US MSAs, aggregate US housing returns and asymmetric volatility. *Advances in Decision Sciences 22*, 1–26.

Phillips, P. and P. Perron (1988). Testing for a unit root in time series regression. *Biometrika 75*, 335–346.

Shiller, R. (1998). *Macro Markets: Creating Institutions for Managing Society's Largest Economic Risks*. New York, NY: Oxford University Press.

Shiryaev, A. (1995). *Probability (Graduate Texts in Mathematics)* (2n Edition ed.). Springer Verlag.

Teraesvirta, T., C. F. Liu, and C. W. J. Granger (1993). Power of the neural network linearity test. *Journal of Time Series Analysis 14*, 209–220.

Wang, W. (2014). *Daily house price indexes: Volatility dynamics and longer-run predictions*. Ph. D. thesis, Duke University. Available for download from: https://dukespace.lib.duke.edu/dspace/handle/10161/8694.

Weron, R. (2002). Estimating long-range dependence: finite sample properties and confidence intervals. *Physica A: Statistical Mechanics and its Applications 312*, 285–299.

White, H. (2000). A reality check for data snooping. *Econometrica 68*, 1097–1126.

Wooldridge, J. (1994). *Aspects of Modelling Nonlinear Time Series*, Chapter Estimation and Inference for Dependent Processes, pp. 2639–2738. Elsevier Science: Amsterdam.

Zhou, Y. and D. R. Haurin (2010). On the determinants of house value volatility. *The Journal of Real Estate Research 32*, 377–396.

Tables and Figures

Table 1: Daily descriptive statistics

	Boston	Chicago	Denver	Los Angeles	Las Vegas	Miami	New York	San Diego	San Francisco	Washington D.C.	Aggregate index	House price futures
No of Obs	4424	3265	3344	4425	4399	3587	4163	4442	4442	2816	2806	2790
Returns												
Mean	1.721E-4	9.291E-6	9.898E-5	1.721E-4	1.098E-5	1.331E-4	1.696E-4	2.175E-4	1.594E-4	1.528E-4	9.811E-5	2.355E-5
SD	3.995E-3	5.933E-3	3.302E-3	3.812E-3	5.686E-3	5.051E-3	3.799E-3	4.106E-3	5.296E-3	5.057E-3	1.627E-32	3.417E-3
Skewness	-1.119	0.131	-0.823	-0.510	-1.613	0.085	-0.041	-0.179	-0.955	-0.192	-0.211	0.847
Kurtosis	18.344	13.417	20.027	6.015	28.151	6.950	19.231	4.916	9.036	6.824	3.770	104.283
Hurst exponent	0.480	0.465	0.532	0.575	0.588***	0.554	0.499	0.559	0.603***	0.544	0.802***	0.775***
Hurst exponent^2	0.751	0.825	0.778	0.848	0.745	0.826	0.795	0.723	0.761	0.823	0.676	0.775
Hurst exponent$_{abs}$	0.724	0.813	0.752	0.807	0.728	0.812	0.778	0.709	0.745	0.803	0.669	0.673
Tail index	3.595	4.182	2.696	3.350	4.141	4.170	3.117	4.996	3.629	4.006	5.922	5.042
Test for dependency and normality												
LB(8)	39.008	24.934	11.918	43.951	36.467	21.984	22.909	9.477	138.048	26.117	335.500	17.805
	(0.000)	(0.002)	(0.155)	(0.000)	(0.000)	(0.005)	(0.004)	(0.304)	(0.000)	(0.001)	(0.000)	(0.023)
Arch(1)	32.834	17.076	206.938	12.622	137.564	104.074	30.273	11.373	6.814	53.604	4.757	0.808
JB	4.432E+4	1.477E+4	4.077E+4	1.178E+5	1.868E+3	2.337E+3	4.876E+4	659.067	7.386E+3	1.734E+3	90.064	1.193E+6
Test for unit root and stationarity												
ADF	-46.334	-38.895	-38.267	-46.131	-46.904	-40.947	-45.888	-45.055	-48.447	-38.353	-66.538	-36.348
PP	-64.349	-56.503	-55.473	-65.475	-68.550	-60.874	-65.931	-65.024	-71.134	-54.086	-99.830	-51.828
KPSS	0.183	0.063	0.133	0.431	0.721	0.438	0.248	0.377	0.295	0.411	0.032	0.262
Test for nonlinearity												
White test	3.170	0.616	6.864	2.295	9.281	13.243	9.249	1.172	9.316	7.495	15.854	14.283
	(0.205)	(0.735)	(0.032)	(0.317)	(0.010)	(0.001)	(0.001)	(0.557)	(0.009)	(0.023)	(0.000)	(0.001)
Teraesvirta test	5.701	15.314	68.878	4.796	0.381	23.922	15.935	4.579	1.647	17.728	12.855	5.819
	(0.058)	(0.000)	(0.000)	(0.091)	(0.827)	(0.000)	(0.000)	(0.101)	(0.439)	(0.000)	(0.002)	(0.055)

Note: *** indicates 1% significance of Hurst coefficients based on the simulated boundary values of Weron (2002) for Wiener Brownian motion. The values in parentheses are the p-values of Ljung-Box test, white and Teraesvirta neutral network tests for nonlinearity.

References

Table 2: The results of RMSE, MAE and MVAR

Models	RMSE			MAE			MVaR			SMVaR		
Horizons	h=1	h=10	h=20	h=1	h=10	h=20	h=1	h=10	h=20	h=1	h=10	h=20
Boston												
GARCH	0.032	0.034	0.034	0.017	0.017	0.017	0.115	0.142	0.143	0.115	0.142	0.144
GJR	0.033	0.034	0.034	0.017	0.017	0.017	0.110	0.143	0.144	0.109	0.142	0.144
EGARCH	0.033	0.034	0.034	0.017	0.018	0.018	0.115	0.134	0.135	0.115	0.134	0.134
APARCH	0.033	0.034	0.034	0.017	0.018	0.018	0.126	0.134	0.136	0.126	0.134	0.135
FIGARCH	0.033	0.035	0.034	0.015	0.016	0.016	0.122	0.169	0.170	0.122	0.168	0.169
MSM	0.031	0.034	0.034	0.015	0.017	0.017	0.107	0.133	0.133	0.106	0.133	0.133
Chicago												
GARCH	0.177	0.192	0.191	0.062	0.068	0.068	0.200	0.279	0.284	0.200	0.279	0.284
GJR	0.178	0.191	0.191	0.062	0.069	0.069	0.194	0.279	0.284	0.193	0.278	0.284
EGARCH	0.182	0.189	0.189	0.061	0.066	0.067	0.215	0.264	0.277	0.215	0.264	0.277
APARCH	0.179	0.192	0.191	0.061	0.066	0.066	0.228	0.301	0.309	0.227	0.301	0.308
FIGARCH	0.190	0.193	0.194	0.055	0.057	0.057	0.320	0.501	0.597	0.320	0.500	0.596
MSM	0.181	0.189	0.190	0.055	0.060	0.059	0.204	0.267	0.282	0.204	0.267	0.282
Denver												
GARCH	0.023	0.023	0.062	0.010	0.011	0.012	0.077	0.085	0.119	0.077	0.085	0.119
GJR	0.022	0.023	0.062	0.010	0.011	0.012	0.077	0.085	0.120	0.077	0.085	0.119
EGARCH	0.023	0.023	0.062	0.010	0.011	0.012	0.082	0.087	0.119	0.082	0.086	0.118
APARCH	0.023	0.023	0.062	0.011	0.011	0.013	0.087	0.087	0.117	0.087	0.086	0.116
FIGARCH	0.023	0.024	0.062	0.010	0.010	0.012	0.078	0.085	0.119	0.077	0.084	0.119
MSM	0.022	0.024	0.062	0.010	0.011	0.013	0.084	0.092	0.122	0.084	0.092	0.122
Las Vegas												
GARCH	0.039	0.040	0.040	0.019	0.020	0.020	0.118	0.143	0.153	0.118	0.143	0.153
GJR	0.040	0.040	0.040	0.020	0.020	0.021	0.116	0.144	0.154	0.115	0.143	0.154
EGARCH	0.041	0.040	0.040	0.021	0.021	0.021	0.134	0.144	0.149	0.134	0.143	0.149
APARCH	0.041	0.039	0.040	0.020	0.020	0.020	0.143	0.141	0.149	0.142	0.141	0.149
FIGARCH	0.042	0.040	0.040	0.016	0.016	0.016	0.176	0.196	0.212	0.175	0.196	0.211
MSM	0.038	0.040	0.040	0.018	0.021	0.021	0.118	0.142	0.146	0.118	0.142	0.146
Los Angeles												
GARCH	0.024	0.025	0.027	0.015	0.016	0.016	0.102	0.117	0.128	0.102	0.117	0.128
GJR	0.024	0.025	0.027	0.016	0.016	0.016	0.107	0.118	0.126	0.107	0.118	0.126
EGARCH	0.025	0.025	0.027	0.017	0.017	0.017	0.108	0.116	0.124	0.108	0.116	0.124
APARCH	0.026	0.062	0.135	0.015	0.050	0.106	0.122	0.192	0.248	0.121	0.192	0.248
FIGARCH	0.026	0.027	0.028	0.015	0.015	0.015	0.134	0.155	0.174	0.133	0.154	0.174
MSM	0.024	0.025	0.027	0.015	0.016	0.016	0.102	0.115	0.124	0.102	0.115	0.124

Note: The entries are RMSE, MAE, and MVaR(5%) and MSVaR(5%) for all six models. For $\nu \geq 6950$ the differences between the non-differentiable and differentiable VaR-based loss functions are vanishing. All the numbers reported here have to be multiplied by 10^{-3}.

Table 3: The results of RMSE, MAE and MVAR

Models	RMSE			MAE			MVaR			SMVaR		
Horizons	h=1	h=10	h=20	h=1	h=10	h=20	h=1	h=10	h=20	h=1	h=10	h=20
Miami												
GARCH	0.042	0.045	0.045	0.027	0.029	0.029	0.128	0.147	0.155	0.128	0.147	0.154
GJR	0.042	0.045	0.045	0.027	0.029	0.029	0.125	0.144	0.156	0.125	0.144	0.155
EGARCH	0.044	0.045	0.045	0.029	0.029	0.029	0.132	0.139	0.143	0.132	0.139	0.143
APARCH	0.045	0.045	0.045	0.028	0.028	0.028	0.145	0.146	0.146	0.145	0.146	0.146
FIGARCH	0.047	0.048	0.048	0.026	0.026	0.026	0.215	0.237	0.263	0.214	0.236	0.262
MSM	0.041	0.045	0.045	0.026	0.028	0.028	0.130	0.142	0.142	0.130	0.142	0.142
New York												
GARCH	0.016	0.017	0.018	0.010	0.010	0.011	0.082	0.098	0.103	0.082	0.098	0.103
GJR	0.016	0.017	0.019	0.010	0.011	0.011	0.084	0.098	0.104	0.084	0.098	0.103
EGARCH	0.017	0.017	0.019	0.010	0.011	0.011	0.088	0.097	0.102	0.088	0.097	0.102
APARCH	0.016	0.017	0.018	0.010	0.010	0.011	0.087	0.098	0.103	0.087	0.098	0.103
FIGARCH	0.017	0.018	0.019	0.009	0.009	0.009	0.096	0.116	0.132	0.096	0.115	0.131
MSM	0.016	0.017	0.018	0.010	0.011	0.011	0.086	0.099	0.101	0.086	0.099	0.101
San Diego												
GARCH	0.032	0.033	0.033	0.019	0.019	0.019	0.107	0.132	0.135	0.107	0.132	0.135
GJR	0.032	0.033	0.033	0.019	0.019	0.019	0.107	0.132	0.133	0.107	0.132	0.132
EGARCH	0.033	0.033	0.033	0.020	0.020	0.020	0.123	0.131	0.131	0.123	0.130	0.131
APARCH	0.033	0.056	0.108	0.019	0.041	0.073	0.129	0.156	0.185	0.129	0.156	0.185
FIGARCH	0.033	0.033	0.033	0.018	0.018	0.018	0.133	0.139	0.140	0.133	0.138	0.140
MSM	0.032	0.033	0.033	0.019	0.019	0.019	0.113	0.129	0.130	0.113	0.129	0.130
San Francisco												
GARCH	0.081	0.083	0.084	0.042	0.043	0.042	0.216	0.259	0.258	0.216	0.258	0.258
GJR	0.081	0.083	0.084	0.043	0.043	0.042	0.209	0.252	0.253	0.209	0.251	0.253
EGARCH	0.082	0.083	0.083	0.045	0.046	0.046	0.216	0.229	0.227	0.216	0.229	0.227
APARCH	0.082	0.083	0.083	0.045	0.045	0.045	0.232	0.235	0.236	0.232	0.235	0.236
FIGARCH	0.086	0.086	0.088	0.039	0.038	0.038	0.404	0.429	0.454	0.404	0.429	0.453
MSM	0.078	0.083	0.084	0.039	0.042	0.041	0.177	0.237	0.248	0.176	0.237	0.248
Washington D.C.												
GARCH	0.042	0.044	0.043	0.026	0.028	0.027	0.132	0.161	0.163	0.132	0.161	0.163
GJR	0.042	0.044	0.043	0.027	0.028	0.028	0.130	0.162	0.160	0.130	0.162	0.159
EGARCH	0.043	0.044	0.043	0.027	0.029	0.028	0.139	0.160	0.160	0.138	0.160	0.159
APARCH	0.044	0.045	0.043	0.026	0.027	0.027	0.156	0.163	0.161	0.156	0.162	0.161
FIGARCH	0.045	0.046	0.045	0.024	0.024	0.024	0.177	0.236	0.251	0.177	0.236	0.250
MSM	0.041	0.044	0.043	0.025	0.027	0.027	0.134	0.153	0.154	0.134	0.153	0.154

Note: Note: The entries are RMSE, MAE, and MVaR(5%) and MSVaR(5%) for all six models. For $\nu \geq 6950$ the differences between the non-differentiable and differentiable VaR-based loss functions are vanishing. All the numbers reported here have to be multiplied by 10^{-3}.

Table 4: The results of RMSE, MAE and MVAR

Models	RMSE			MAE			MVaR			SMVaR		
Horizons	h=1	h=10	h=20	h=1	h=10	h=20	h=1	h=10	h=20	h=1	h=10	h=20
Aggregate index												
GARCH	0.005	0.006	0.006	0.003	0.003	0.003	0.046	0.066	0.068	0.045	0.064	0.067
GJR	0.005	0.006	0.006	0.003	0.003	0.003	0.044	0.064	0.067	0.043	0.063	0.065
EGARCH	0.006	0.006	0.006	0.004	0.004	0.004	0.047	0.050	0.051	0.046	0.049	0.051
APARCH	0.006	0.019	0.043	0.003	0.015	0.035	0.150	0.159	0.183	0.147	0.158	0.182
FIGARCH	0.006	0.006	0.006	0.003	0.003	0.003	0.071	0.077	0.082	0.069	0.075	0.080
MSM	0.005	0.006	0.006	0.003	0.003	0.003	0.047	0.054	0.058	0.046	0.053	0.057
House price futures												
GARCH	0.103	0.106	0.106	0.019	0.019	0.019	0.085	0.086	0.086	0.085	0.086	0.086
GJR	0.098	0.106	0.106	0.018	0.019	0.019	0.085	0.087	0.087	0.085	0.087	0.087
EGARCH	2.719	0.509	0.476	0.165	0.049	0.047	0.121	0.097	0.097	0.121	0.097	0.097
APARCH	0.100	0.302	0.182	0.019	0.111	0.063	0.085	0.168	0.139	0.085	0.168	0.139
FIGARCH	0.079	0.107	0.108	0.016	0.028	0.029	0.089	0.109	0.114	0.087	0.109	0.114
MSM	0.099	0.107	0.106	0.010	0.014	0.015	0.038	0.084	0.085	0.038	0.084	0.085

Note: Note: The entries are RMSE, MAE, and MVaR(5%) and MSVaR(5%) for all six models. For $\nu \geq 6950$ the differences between the non-differentiable and differentiable VaR-based loss functions are vanishing. All the numbers reported here have to be multiplied by 10^{-3}.

Table 5: MCS test results using squared and absolute loss functions

Squared loss function						Absolute loss function					
Horizons											
h=1		h=10		h=20		h=1		h=10		h=20	
Model	pv_{MCS}	Model	pv_{MCS}	Model	pv_{MCS}	Model	pv_{MCS}	Model	pv_{MCS}	Model	pv_{MCS}
Boston											
FIGARCH	0.000	FIGARCH	0.006	FIGARCH	0.015	EGARCH	0.000	EGARCH	0.000	EGARCH	0.000
EGARCH	0.000	GJR	0.204*	GARCH	0.682*	APARCH	0.000	APARCH	0.000	APARCH	0.000
APARCH	0.000	GARCH	0.249*	MSM	0.736*	GJR	0.000	GJR	0.000	GJR	0.000
GARCH	0.000	MSM	0.274*	GJR	0.736*	GARCH	0.000	MSM	0.000	MSM	0.000
GJR	0.000	APARCH	0.274*	APARCH	0.736*	MSM	0.963*	GARCH	0.000	GARCH	0.000
MSM	1.000*	EGARCH	1.000*	EGARCH	1.000*	FIGARCH	1.000*	FIGARCH	1.000*	FIGARCH	1.000*
Chicago											
FIGARCH	0.030	FIGARCH	0.003	FIGARCH	0.000	EGARCH	0.000	EGARCH	0.000	EGARCH	0.000
EGARCH	0.348*	APARCH	0.099	APARCH	0.123*	GJR	0.002	GJR	0.001	GJR	0.001
MSM	0.433*	GJR	0.099	GJR	0.123*	GARCH	0.002	GARCH	0.001	GARCH	0.001
APARCH	0.433*	GARCH	0.127*	GARCH	0.123*	APARCH	0.002	APARCH	0.001	APARCH	0.001
GJR	0.614*	MSM	0.678*	MSM	0.474*	FIGARCH	0.849*	MSM	0.001	MSM	0.006
GARCH	1.000*	EGARCH	1.000*	EGARCH	1.000*	MSM	1.000*	FIGARCH	1.000*	FIGARCH	1.000*
Denver											
EGARCH	0.000	FIGARCH	0.438*	FIGARCH	0.187*	APARCH	0.000	MSM	0.000	MSM	0.000
FIGARCH	0.000	MSM	0.832*	GJR	0.783*	EGARCH	0.000	APARCH	0.000	APARCH	0.000
APARCH	0.000	GARCH	0.832*	GARCH	0.830*	GARCH	0.000	GARCH	0.000	GARCH	0.057
GARCH	0.000	APARCH	0.984*	MSM	0.830*	GJR	0.000	EGARCH	0.002	EGARCH	0.151*
GJR	0.000	GJR	0.984*	EGARCH	0.830*	FIGARCH	0.001	GJR	0.002	GJR	0.151*
MSM	1.000*	EGARCH	1.000*	APARCH	1.000*	MSM	1.000*	FIGARCH	1.000*	FIGARCH	1.000*
Las Vegas											
APARCH	0.001	EGARCH	0.063	EGARCH	0.076	EGARCH	0.000	MSM	0.000	MSM	0.000
EGARCH	0.001	GJR	0.499*	GJR	0.246*	APARCH	0.000	EGARCH	0.000	EGARCH	0.000
FIGARCH	0.001	FIGARCH	0.586*	FIGARCH	0.445*	GARCH	0.000	GARCH	0.000	GJR	0.000
GJR	0.001	GARCH	0.586*	GARCH	0.445*	GJR	0.000	APARCH	0.000	GARCH	0.000
GARCH	0.001	MSM	0.586*	MSM	0.547*	MSM	0.000	GJR	0.000	APARCH	0.000
MSM	1.000*	APARCH	1.000*	APARCH	1.000*	FIGARCH	1.000*	FIGARCH	1.000*	FIGARCH	1.000*
Los Angeles											
FIGARCH	0.000	APARCH	0.000	APARCH	0.000	EGARCH	0.000	APARCH	0.000	APARCH	0.000
APARCH	0.000	FIGARCH	0.000	FIGARCH	0.000	GJR	0.000	EGARCH	0.000	EGARCH	0.000
EGARCH	0.000	GJR	0.366*	GARCH	0.231*	GARCH	0.007	GARCH	0.000	GARCH	0.000
GJR	0.004	GARCH	0.366*	GJR	0.377*	APARCH	0.007	GJR	0.000	MSM	0.000
GARCH	0.410*	MSM	0.748*	MSM	0.509*	MSM	0.041	MSM	0.000	GJR	0.000
MSM	1.000*	EGARCH	1.000*	EGARCH	1.000*	FIGARCH	1.000*	FIGARCH	1.000*	FIGARCH	1.000*

Note: MCS p-values for forecasts from six volatility models at different forecasting horizons. The p-values are computed via a stationary bootstrap (B=10000) using the range statistic T_r. The forecasts in $\mathcal{M}^*_{95\%}$ are identified by one asterisk.

Table 6: MCS test results using squared and absolute loss functions

Squared loss function						Absolute loss function					
Horizons											
h=1		h=10		h=20		h=1		h=10		h=20	
Model	pv_{MCS}	Model	pv_{MCS}	Model	pv_{MCS}	Model	pv_{MCS}	Model	pv_{MCS}	Model	pv_{MCS}
Miami											
FIGARCH	0.000	FIGARCH	0.000	FIGARCH	0.000	EGARCH	0.000	EGARCH	0.000	EGARCH	0.000
EGARCH	0.000	GARCH	0.144*	GARCH	0.080	APARCH	0.000	GJR	0.000	GJR	0.000
APARCH	0.000	APARCH	0.280*	GJR	0.310*	GARCH	0.000	GARCH	0.000	GARCH	0.000
GARCH	0.000	GJR	0.872*	APARCH	0.749*	GJR	0.000	MSM	0.000	APARCH	0.000
GJR	0.000	MSM	0.872*	MSM	0.749*	FIGARCH	0.956*	APARCH	0.000	MSM	0.001
MSM	1.000*	EGARCH	1.000*	EGARCH	1.000*	MSM	1.000*	FIGARCH	1.000*	FIGARCH	1.000*
New York											
EGARCH	0.000	FIGARCH	0.280*	FIGARCH	0.048	EGARCH	0.000	MSM	0.000	MSM	0.000
FIGARCH	0.000	EGARCH	0.568*	GJR	0.091	APARCH	0.000	EGARCH	0.000	EGARCH	0.000
APARCH	0.000	GJR	0.770*	EGARCH	0.155*	GJR	0.000	GJR	0.000	GJR	0.000
GARCH	0.000	APARCH	0.963*	APARCH	0.566*	GARCH	0.000	APARCH	0.000	APARCH	0.000
GJR	0.000	MSM	0.963*	GARCH	0.755*	MSM	0.000	GARCH	0.000	GARCH	0.000
MSM	1.000*	GARCH	1.000*	MSM	1.000*	FIGARCH	1.000*	FIGARCH	1.000*	FIGARCH	1.000*
San Diego											
APARCH	0.000	APARCH	0.000	APARCH	0.000	EGARCH	0.000	APARCH	0.000	APARCH	0.000
EGARCH	0.000	FIGARCH	0.007	FIGARCH	0.000	APARCH	0.002	EGARCH	0.000	EGARCH	0.000
FIGARCH	0.000	GJR	0.011	GJR	0.125*	GJR	0.002	MSM	0.000	MSM	0.000
GJR	0.020	GARCH	0.103*	EGARCH	0.346*	GARCH	0.077	GJR	0.000	GJR	0.000
GARCH	0.024	EGARCH	0.105*	GARCH	0.346*	MSM	0.344*	GARCH	0.000	GARCH	0.000
MSM	1.000*	MSM	1.000*	MSM	1.000*	FIGARCH	1.000*	FIGARCH	1.000*	FIGARCH	1.000*
San Francisco											
FIGARCH	0.000	FIGARCH	0.000	FIGARCH	0.000	APARCH	0.000	EGARCH	0.000	EGARCH	0.000
APARCH	0.000	MSM	0.260*	MSM	0.051	EGARCH	0.000	APARCH	0.000	APARCH	0.000
EGARCH	0.000	GARCH	0.260*	GARCH	0.101	GJR	0.000	GJR	0.000	GJR	0.000
GARCH	0.000	GJR	0.260*	GJR	0.364*	GARCH	0.000	GARCH	0.000	GARCH	0.000
GJR	0.000	APARCH	0.844*	APARCH	0.742*	MSM	0.328*	MSM	0.000	MSM	0.000
MSM	1.000*	EGARCH	1.000*	EGARCH	1.000*	FIGARCH	1.000*	FIGARCH	1.000*	FIGARCH	1.000*
Washington D. C.											
FIGARCH	0.000	FIGARCH	0.000	FIGARCH	0.000	EGARCH	0.000	GJR	0.000	EGARCH	0.000
APARCH	0.000	APARCH	0.169*	APARCH	0.276*	GJR	0.000	EGARCH	0.000	GJR	0.000
EGARCH	0.000	EGARCH	0.550*	EGARCH	0.389*	GARCH	0.000	MSM	0.000	GARCH	0.000
GARCH	0.000	GJR	0.599*	GARCH	0.389*	APARCH	0.001	GARCH	0.000	MSM	0.000
GJR	0.000	GARCH	0.599*	GJR	0.649*	MSM	0.001	APARCH	0.001	APARCH	0.001
MSM	1.000*	MSM	1.000*	MSM	1.000*	FIGARCH	1.000*	FIGARCH	1.000*	FIGARCH	1.000*

Note: MCS p-values for forecasts from six volatility models at different forecasting horizons. The p-values are computed via a stationary bootstrap (B=10000) using the range statistic T_r. The forecasts in $\mathcal{M}^*_{95\%}$ are identified by one asterisk.

Table 7: MCS test results using squared and absolute loss functions

Squared loss function						Absolute loss function					
Horizons											
h=1		h=10		h=20		h=1		h=10		h=20	
Model	pv_{MCS}	Model	pv_{MCS}	Model	pv_{MCS}	Model	pv_{MCS}	Model	pv_{MCS}	Model	pv_{MCS}
Aggregate index											
APARCH	0.000	APARCH	0.000	APARCH	0.000	EGARCH	0.000	APARCH	0.000	APARCH	0.000
FIGARCH	0.000	FIGARCH	0.000	FIGARCH	0.000	APARCH	0.000	EGARCH	0.000	EGARCH	0.000
EGARCH	0.002	GARCH	0.000	GARCH	0.000	MSM	0.000	MSM	0.000	MSM	0.000
MSM	0.174*	GJR	0.000	GJR	0.000	FIGARCH	0.015	GARCH	0.002	GARCH	0.011
GJR	0.174*	MSM	0.006	MSM	0.002	GARCH	0.485*	GJR	0.002	GJR	0.011
GARCH	1.000*	EGARCH	1.000*	EGARCH	1.000*	GJR	1.000*	FIGARCH	1.000*	FIGARCH	1.000*
House price futures											
EGARCH	0.042	EGARCH	0.004	EGARCH	0.012	EGARCH	0.000	APARCH	0.000	APARCH	0.000
GARCH	0.042	APARCH	0.004	APARCH	0.012	APARCH	0.000	EGARCH	0.000	EGARCH	0.000
APARCH	0.269*	FIGARCH	0.022	FIGARCH	0.029	GARCH	0.000	FIGARCH	0.000	FIGARCH	0.000
MSM	0.269*	MSM	0.748*	GARCH	0.671*	GJR	0.000	GJR	0.000	GJR	0.000
GJR	0.269*	GARCH	0.748*	MSM	0.980*	FIGARCH	0.000	GARCH	0.000	GARCH	0.000
FIGARCH	1.000*	GJR	1.000*	GJR	1.000*	MSM	1.000*	MSM	1.000*	MSM	1.000*

Note: MCS p-values for forecasts from six volatility models at different forecasting horizons. The p-values are computed via a stationary bootstrap (B=10000) using the range statistic T_r. The forecasts in $\mathcal{M}^*_{95\%}$ are identified by one asterisk.

Table 8: MCS test results using VaR-based loss function

Discrete VaR-based loss function						Continuous VaR-based loss function					
Horizons											
h=1		h=10		h=20		h=1		h=10		h=20	
Model	pv_{MCS}	Model	pv_{MCS}	Model	pv_{MCS}	Model	pv_{MCS}	Model	pv_{MCS}	Model	pv_{MCS}
Boston											
APARCH	0.011	FIGARCH	0.012	FIGARCH	0.020	APARCH	0.012	FIGARCH	0.015	FIGARCH	0.018
FIGARCH	0.144*	GJR	0.029	GJR	0.074*	FIGARCH	0.142*	GJR	0.035	GJR	0.065*
EGARCH	0.144*	GARCH	0.085*	GARCH	0.105*	EGARCH	0.142*	GARCH	0.093*	GARCH	0.100*
GARCH	0.144*	APARCH	0.933*	APARCH	0.665*	GARCH	0.142*	APARCH	0.941*	APARCH	0.681*
GJR	0.488*	EGARCH	0.933*	EGARCH	0.665*	GJR	0.491*	EGARCH	0.941*	EGARCH	0.681*
MSM	1.000*	MSM	1.000*	MSM	1.000*	MSM	1.000*	MSM	1.000*	MSM	1.000*
Chicago											
FIGARCH	0.001	FIGARCH	0.000	FIGARCH	0.000	FIGARCH	0.001	FIGARCH	0.000	FIGARCH	0.000
EGARCH	0.129*	APARCH	0.024	APARCH	0.031	EGARCH	0.133*	APARCH	0.019	APARCH	0.036
APARCH	0.161*	GJR	0.024	GJR	0.546*	APARCH	0.173*	GJR	0.019	GJR	0.567*
MSM	0.331*	GARCH	0.024	GARCH	0.546*	MSM	0.336*	GARCH	0.019	GARCH	0.567*
GARCH	0.331*	MSM	0.617*	MSM	0.665*	GARCH	0.336*	MSM	0.595*	MSM	0.671*
GJR	1.000*	EGARCH	1.000*	EGARCH	1.000*	GJR	1.000*	EGARCH	1.000*	EGARCH	1.000*
Denver											
APARCH	0.000	MSM	0.154*	MSM	0.006	APARCH	0.000	MSM	0.146*	MSM	0.005
MSM	0.000	EGARCH	0.926*	GJR	0.776*	MSM	0.000	EGARCH	0.895*	GJR	0.779*
EGARCH	0.022	APARCH	0.926*	GARCH	0.776*	EGARCH	0.020	APARCH	0.895*	GARCH	0.779*
FIGARCH	0.080*	GARCH	0.926*	EGARCH	0.776*	FIGARCH	0.042	GARCH	0.895*	EGARCH	0.779*
GARCH	0.080*	GJR	0.926*	FIGARCH	0.776*	GARCH	0.042	GJR	0.895*	FIGARCH	0.779*
GJR	1.000*	FIGARCH	1.000*	APARCH	1.000*	GJR	1.000*	FIGARCH	1.000*	APARCH	1.000*
Las Vegas											
FIGARCH	0.001	FIGARCH	0.007	FIGARCH	0.005	FIGARCH	0.002	FIGARCH	0.008	FIGARCH	0.006
APARCH	0.001	EGARCH	0.494*	GJR	0.133*	APARCH	0.002	EGARCH	0.514*	GJR	0.126*
EGARCH	0.001	GJR	0.859*	GARCH	0.333*	EGARCH	0.002	GJR	0.843*	GARCH	0.335*
GARCH	0.071	GARCH	0.859*	EGARCH	0.836*	GARCH	0.064*	GARCH	0.843*	EGARCH	0.853*
MSM	0.665*	MSM	0.957*	APARCH	0.836*	MSM	0.644*	MSM	0.932*	APARCH	0.853*
GJR	1.000*	APARCH	1.000*	MSM	1.000*	GJR	1.000*	APARCH	1.000*	MSM	1.000*
Los Angeles											
FIGARCH	0.001	APARCH	0.000	APARCH	0.000	FIGARCH	0.000	APARCH	0.000	APARCH	0.000
APARCH	0.001	FIGARCH	0.004	FIGARCH	0.002	APARCH	0.000	FIGARCH	0.005	FIGARCH	0.002
EGARCH	0.001	GJR	0.782*	GARCH	0.373*	EGARCH	0.000	GJR	0.798*	GARCH	0.417*
GJR	0.578*	GARCH	0.782*	GJR	0.583*	GJR	0.557*	GARCH	0.798*	GJR	0.612*
GARCH	0.876*	EGARCH	0.782*	MSM	0.949*	GARCH	0.901*	EGARCH	0.798*	MSM	0.951*
MSM	1.000*	MSM	1.000*	EGARCH	1.000*	MSM	1.000*	MSM	1.000*	EGARCH	1.000*

Note: MCS p-values for forecasts from six volatility models at different forecasting horizons. The p-values are computed via a stationary bootstrap (B=10000) using the range statistic T_r. The forecasts in $\mathcal{M}^*_{95\%}$ are identified by one asterisk.

Table 9: MCS test results

Discrete VaR-based loss function						Continuous VaR-based loss function					
Horizons											
h=1		h=10		h=20		h=1		h=10		h=20	
Model	pv_{MCS}	Model	pv_{MCS}	Model	pv_{MCS}	Model	pv_{MCS}	Model	pv_{MCS}	Model	pv_{MCS}
Miami											
FIGARCH	0.000	FIGARCH	0.000	FIGARCH	0.000	FIGARCH	0.000	FIGARCH	0.000	FIGARCH	0.000
APARCH	0.002	GARCH	0.390*	GJR	0.133*	APARCH	0.002	GARCH	0.386*	GJR	0.120*
EGARCH	0.002	APARCH	0.410*	GARCH	0.151*	EGARCH	0.002	APARCH	0.419*	GARCH	0.142*
MSM	0.025	GJR	0.410*	APARCH	0.698*	MSM	0.030	GJR	0.419*	APARCH	0.723*
GARCH	0.025	MSM	0.410*	EGARCH	0.698*	GARCH	0.030	MSM	0.419*	EGARCH	0.723*
GJR	1.000*	EGARCH	1.000*	MSM	1.000*	GJR	1.000*	EGARCH	1.000*	MSM	1.000*
New York											
FIGARCH	0.003	FIGARCH	0.186*	FIGARCH	0.029	FIGARCH	0.004	FIGARCH	0.222*	FIGARCH	0.032
EGARCH	0.003	MSM	0.837*	GJR	0.847*	EGARCH	0.004	MSM	0.856*	GJR	0.870*
APARCH	0.012	GARCH	0.837*	APARCH	0.847*	APARCH	0.016	GARCH	0.856*	APARCH	0.870*
MSM	0.087*	GJR	0.837*	GARCH	0.847*	MSM	0.093*	GJR	0.856*	GARCH	0.870*
GJR	0.087*	APARCH	0.837*	EGARCH	0.847*	GJR	0.093*	APARCH	0.856*	EGARCH	0.870*
GARCH	1.000*	EGARCH	1.000*	MSM	1.000*	GARCH	1.000*	EGARCH	1.000*	MSM	1.000*
San Diego											
APARCH	0.032	APARCH	0.044	APARCH	0.004	APARCH	0.037	APARCH	0.049	APARCH	0.004
FIGARCH	0.032	FIGARCH	0.425*	FIGARCH	0.288*	FIGARCH	0.037	FIGARCH	0.484*	FIGARCH	0.336*
EGARCH	0.032	GJR	0.769*	GARCH	0.425*	EGARCH	0.037	GJR	0.773*	GARCH	0.460*
MSM	0.100*	GARCH	0.769*	GJR	0.593*	MSM	0.105*	GARCH	0.773*	GJR	0.622*
GJR	0.715*	EGARCH	0.769*	EGARCH	0.593*	GJR	0.681*	EGARCH	0.773*	EGARCH	0.622*
GARCH	1.000*	MSM	1.000*	MSM	1.000*	GARCH	1.000*	MSM	1.000*	MSM	1.000*
San Francisco											
FIGARCH	0.000	FIGARCH	0.000	FIGARCH	0.000	FIGARCH	0.000	FIGARCH	0.000	FIGARCH	0.000
APARCH	0.000	GARCH	0.001	GARCH	0.003	APARCH	0.000	GARCH	0.002	GARCH	0.002
EGARCH	0.000	GJR	0.003	GJR	0.004	EGARCH	0.000	GJR	0.003	GJR	0.003
GARCH	0.000	MSM	0.024	MSM	0.012	GARCH	0.000	MSM	0.024	MSM	0.012
GJR	0.000	APARCH	0.024	APARCH	0.012	GJR	0.000	APARCH	0.024	APARCH	0.012
MSM	1.000*	EGARCH	1.000*	EGARCH	1.000*	MSM	1.000*	EGARCH	1.000*	EGARCH	1.000*
Washington D. C.											
FIGARCH	0.001	FIGARCH	0.000	FIGARCH	0.000	FIGARCH	0.001	FIGARCH	0.000	FIGARCH	0.000
APARCH	0.001	GJR	0.391*	GARCH	0.322*	APARCH	0.001	GJR	0.390*	GARCH	0.336*
EGARCH	0.001	APARCH	0.391*	APARCH	0.322*	EGARCH	0.001	APARCH	0.390*	APARCH	0.336*
MSM	0.233*	EGARCH	0.391*	EGARCH	0.322*	MSM	0.227*	EGARCH	0.390*	EGARCH	0.336*
GARCH	0.233*	GARCH	0.391*	GJR	0.322*	GARCH	0.227*	GARCH	0.390*	GJR	0.336*
GJR	1.000*	MSM	1.000*	MSM	1.000*	GJR	1.000*	MSM	1.000*	MSM	1.000*

Note: MCS p-values for forecasts from six volatility models at different forecasting horizons. The p-values are computed via a stationary bootstrap (B=10000) using the range statistic T_r. The forecasts in $\mathcal{M}^*_{95\%}$ are identified by one asterisk.

Table 10: MCS test results

Discrete VaR-based loss function						Continuous VaR-based loss function					
Horizons											
h=1		h=10		h=20		h=1		h=10		h=20	
Model	pv_{MCS}	Model	pv_{MCS}	Model	pv_{MCS}	Model	pv_{MCS}	Model	pv_{MCS}	Model	pv_{MCS}
Aggregate index											
APARCH	0.000	APARCH	0.000	APARCH	0.000	APARCH	0.000	APARCH	0.000	APARCH	0.000
FIGARCH	0.000	FIGARCH	0.001	FIGARCH	0.001	FIGARCH	0.001	FIGARCH	0.002	FIGARCH	0.001
MSM	0.025	GARCH	0.017	GARCH	0.004	MSM	0.021	GARCH	0.023	GARCH	0.006
EGARCH	0.068*	GJR	0.017	GJR	0.012	EGARCH	0.084*	GJR	0.023	GJR	0.017
GARCH	0.068*	MSM	0.023	MSM	0.016	GARCH	0.084*	MSM	0.033	MSM	0.020
GJR	1.000*	EGARCH	1.000*	EGARCH	1.000*	GJR	1.000*	EGARCH	1.000*	EGARCH	1.000*
House price futures											
EGARCH	0.000	APARCH	0.000	APARCH	0.000	EGARCH	0.000	APARCH	0.000	APARCH	0.000
APARCH	0.000	FIGARCH	0.000	FIGARCH	0.000	APARCH	0.000	FIGARCH	0.000	FIGARCH	0.000
FIGARCH	0.000	EGARCH	0.012	EGARCH	0.009	FIGARCH	0.000	EGARCH	0.013	EGARCH	0.010
GJR	0.000	GJR	0.051	GJR	0.061	GJR	0.000	GJR	0.057	GJR	0.056
GARCH	0.000	GARCH	0.690*	GARCH	0.731*	GARCH	0.000	GARCH	0.688*	GARCH	0.747*
MSM	1.000*	MSM	1.000*	MSM	1.000*	MSM	1.000*	MSM	1.000*	MSM	1.000*

Note: MCS p-values for forecasts from six volatility models at different forecasting horizons. The p-values are computed via a stationary bootstrap (B=10000) using the range statistic T_r. The forecasts in $\mathcal{M}^*_{95\%}$ are identified by one asterisk.

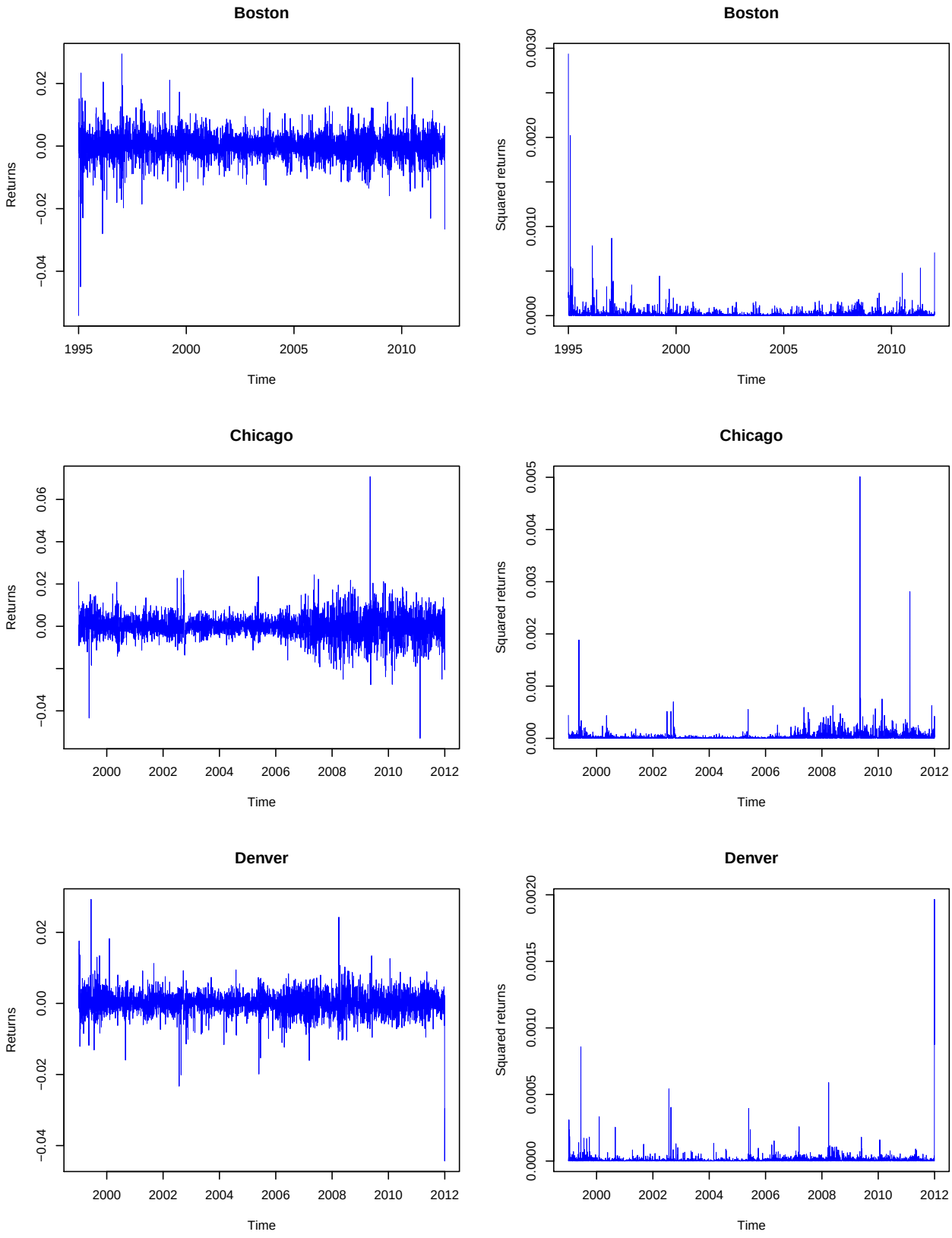

Figure 1: Daily housing returns and squared returns

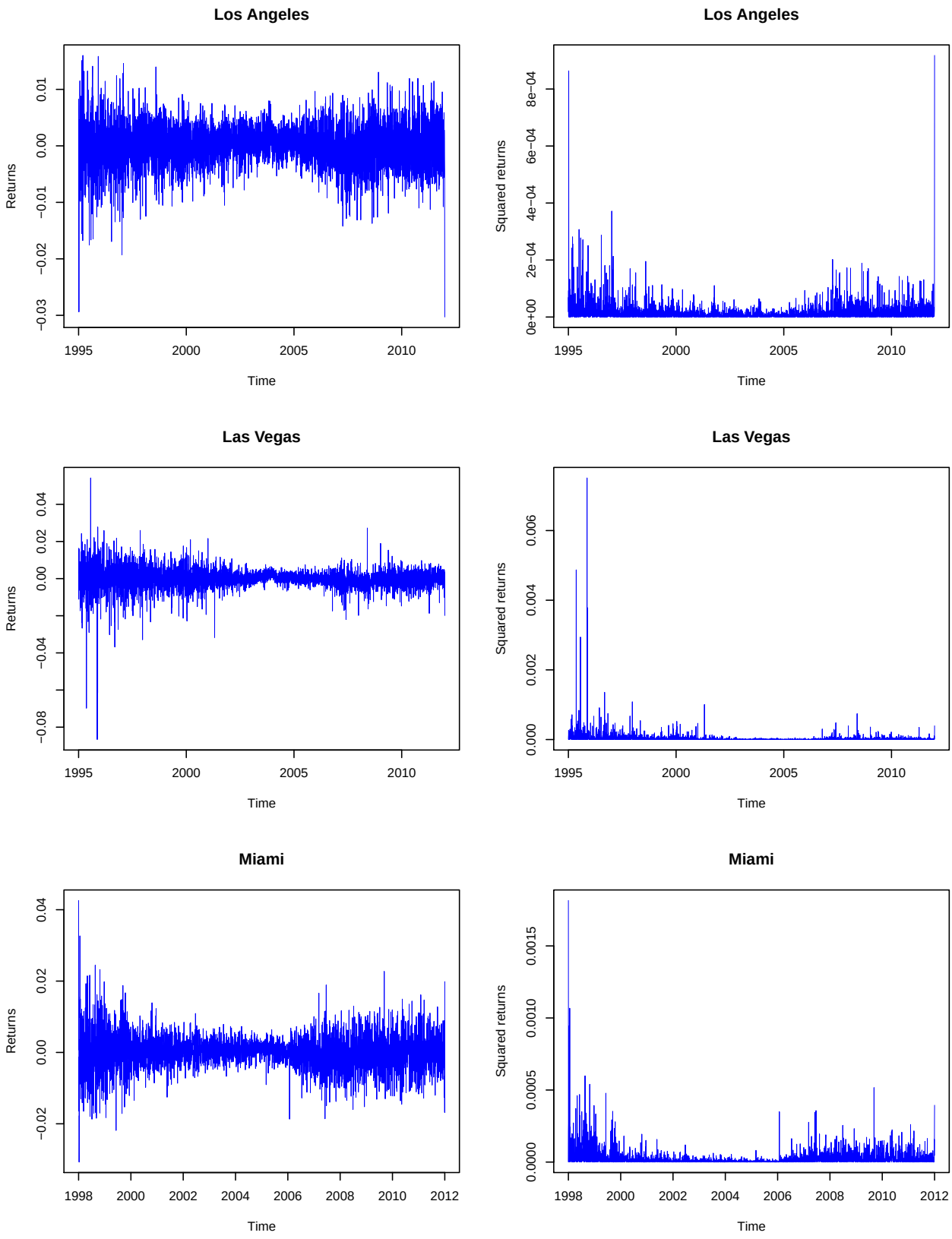

Figure 2: Daily housing returns and squared returns

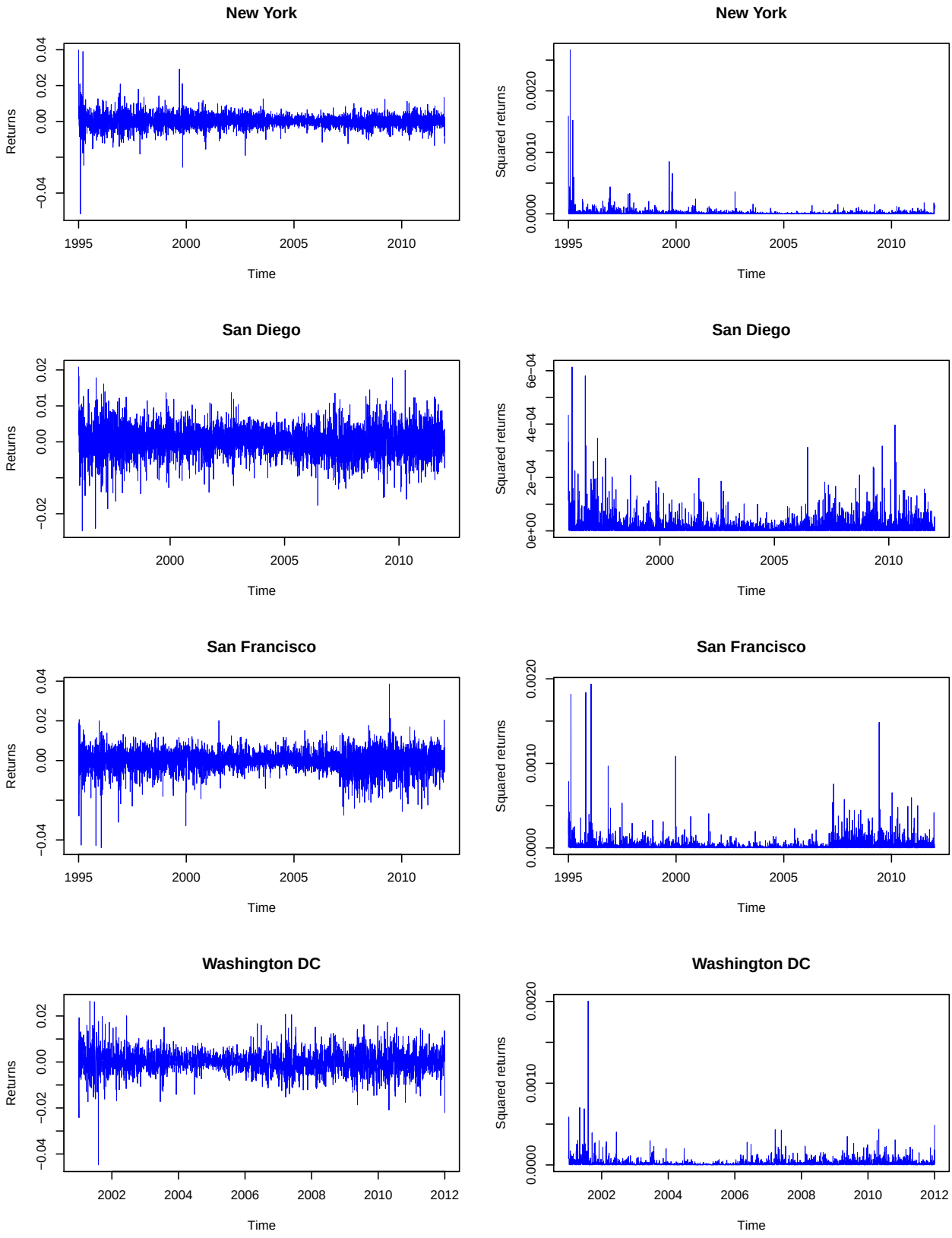

Figure 3: Daily housing returns and squared returns

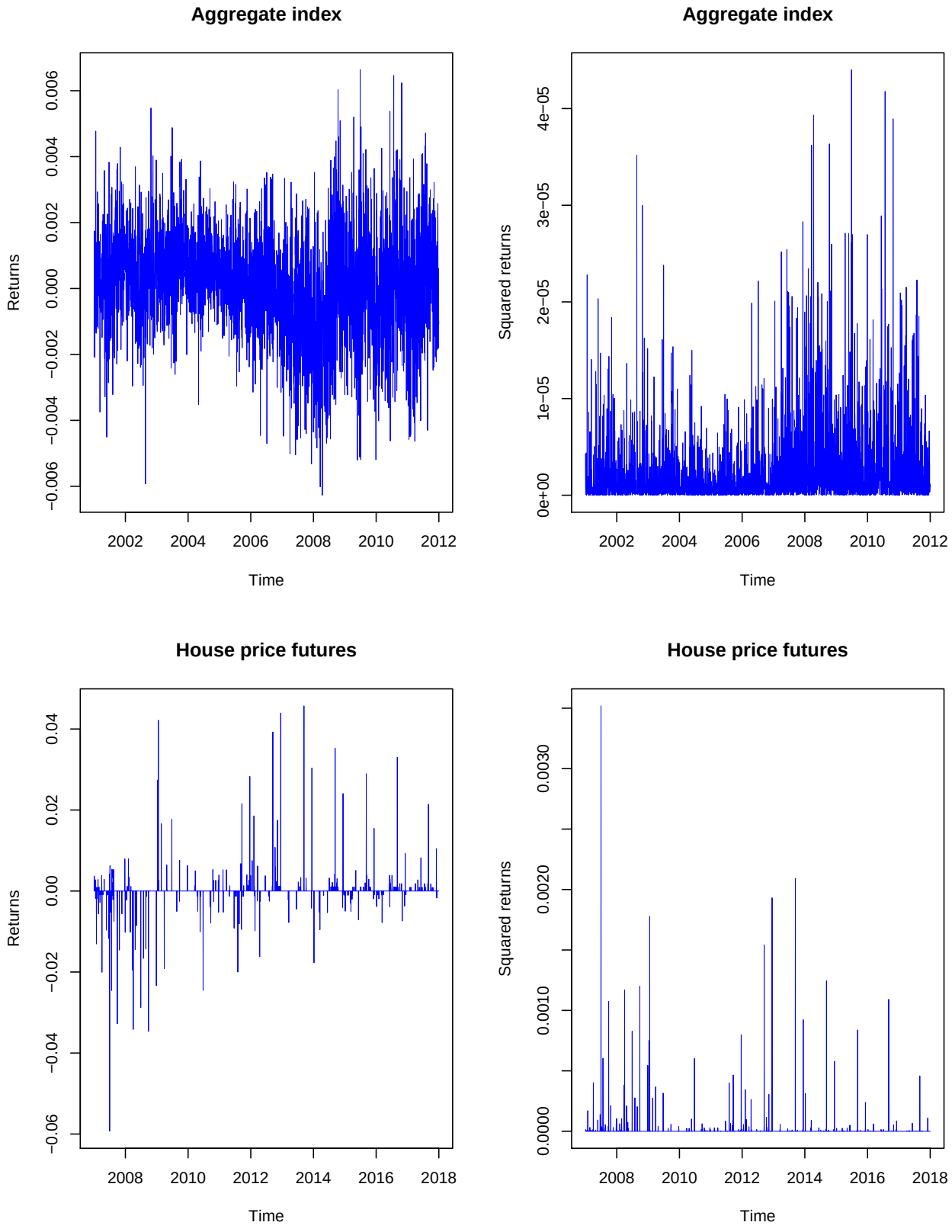

Figure 4: Daily Composite 10 housing price and house price futures index returns and squared returns

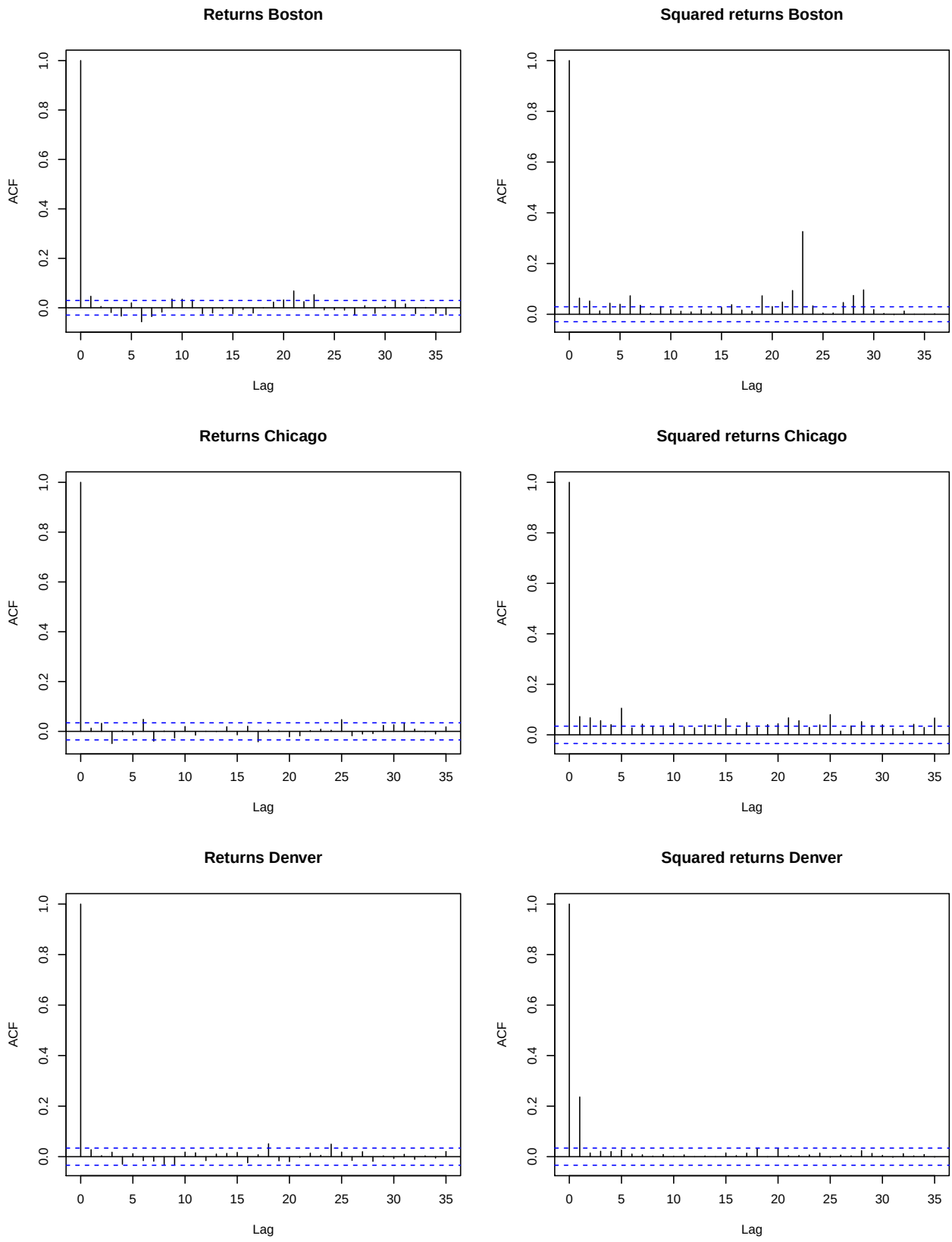

Figure 5: ACFs for housing returns and squared returns

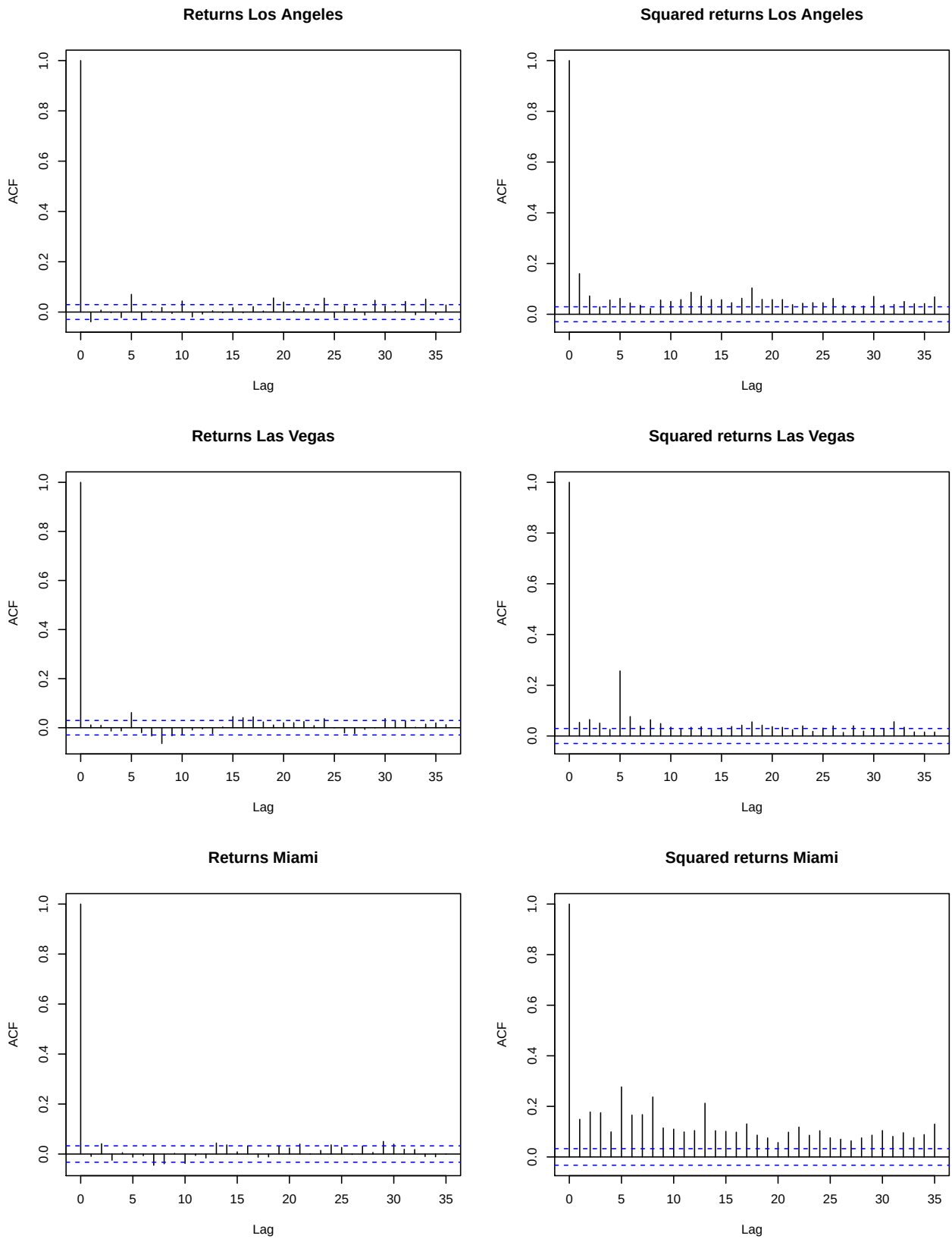

Figure 6: ACFs for housing returns and squared returns

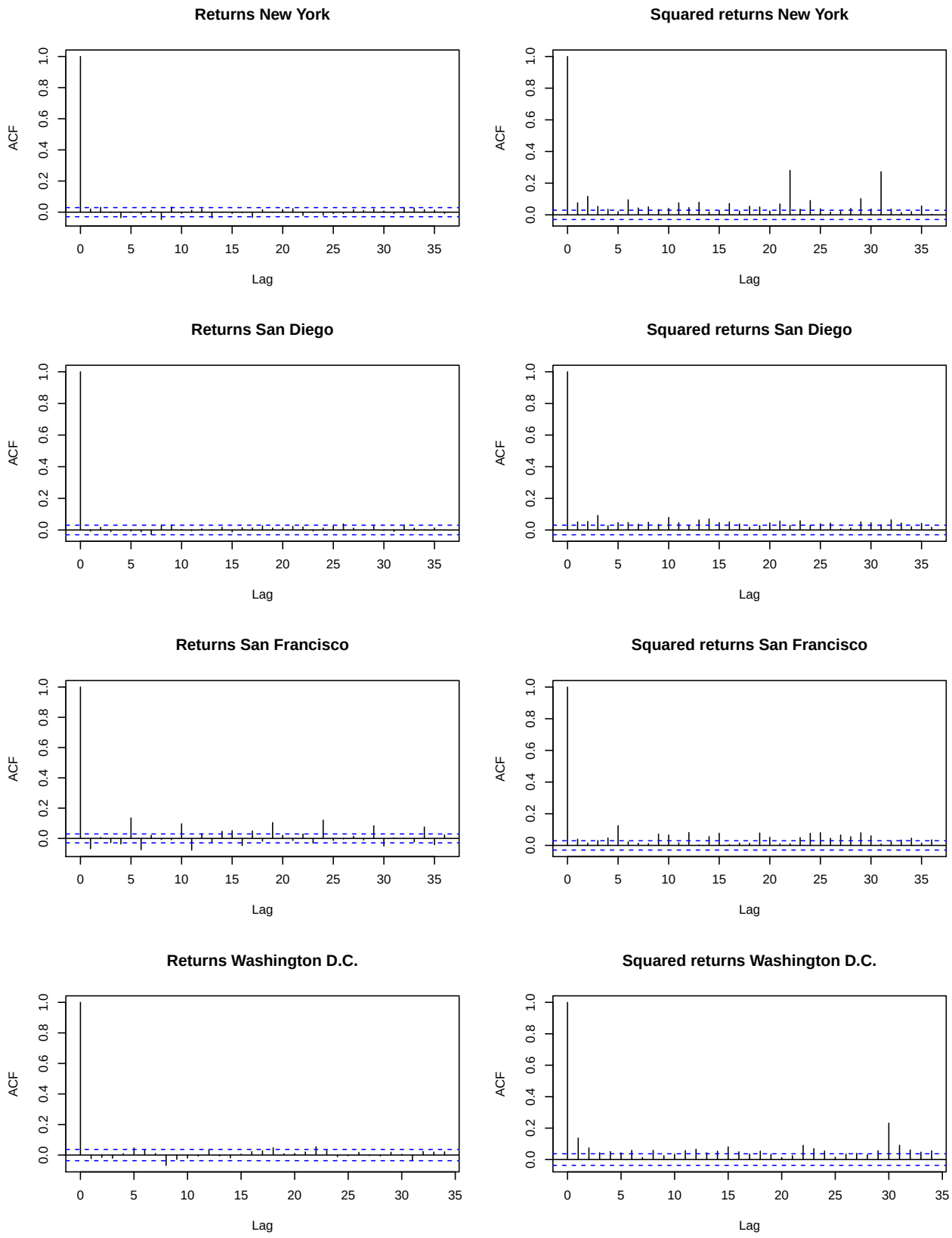

Figure 7: ACFs for housing returns and squared returns

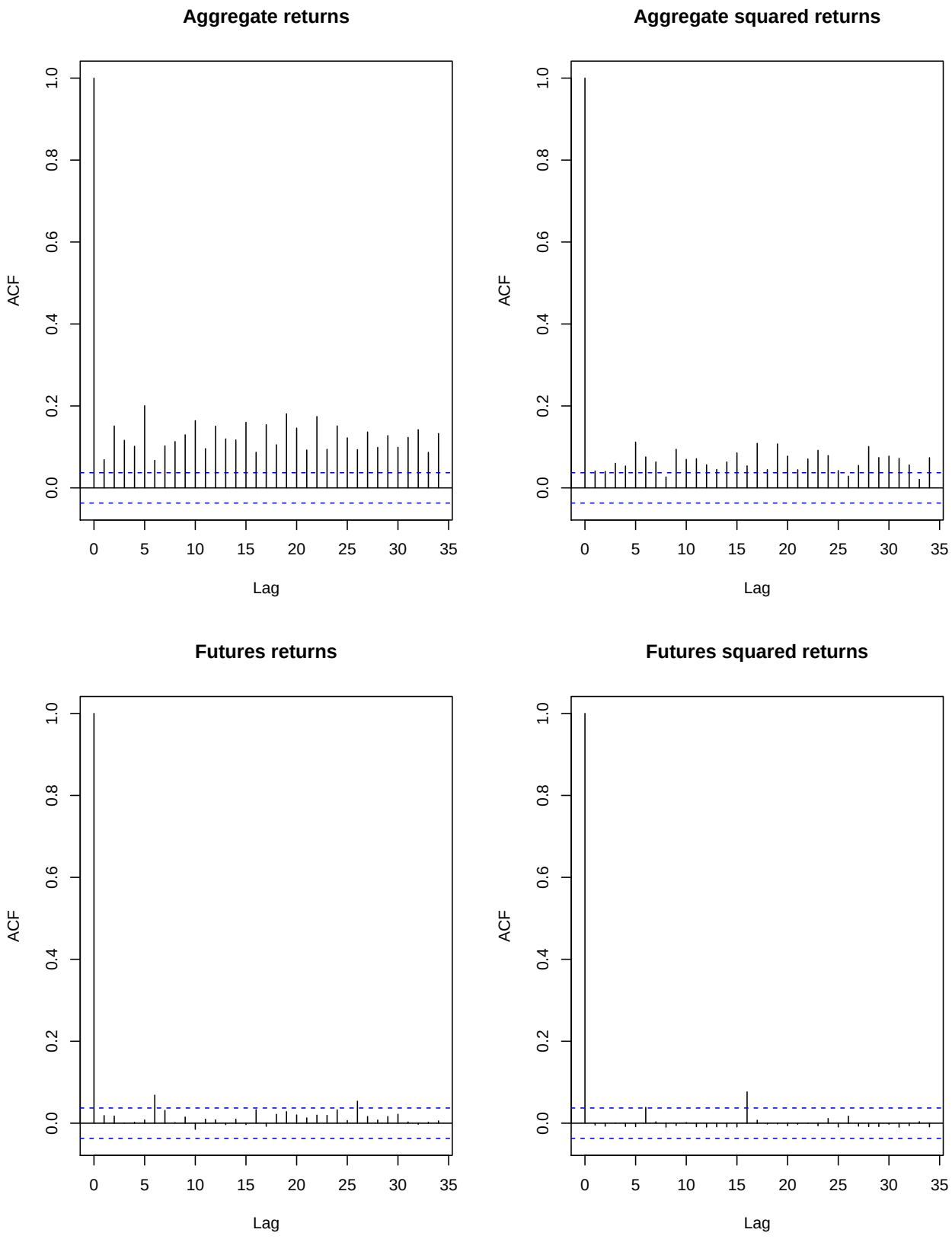

Figure 8: ACFs for daily composite and future housing returns and their squared returns